


Review

Carbon Nanostructures as a Multi-Functional Platform for Sensing Applications

Rafael Gregorio Mendes ^{1,*}, Paweł S. Wróbel ², Alicja Bachmatiuk ², Jingyu Sun ^{3,4}, Thomas Gemming ¹ , Zhongfan Liu ^{3,4,5} and Mark Hermann Rummeli ^{1,2,3,4,*}

¹ Leibniz Institute for Solid State and Materials Research Dresden; Helmholtzstr. 20, 01069 Dresden, Germany; t.gemming@ifw-dresden.de

² Centre of Polymer and Carbon Materials Polish Academy of Sciences; Marie Curie-Skłodowskiej 34 Str., 41-819 Zabrze, Poland; pwrobel@cmpw-pan.edu.pl (P.S.W.); alicja-bachmatiuk@wp.pl (A.B.)

³ Soochow Institute for Energy and Materials Innovations, College of Physics, Optoelectronics and Energy, Collaborative Innovation Center of Suzhou Nano Science and Technology, Soochow University, Suzhou 215006, China; sunjy86@suda.edu.cn (J.S.); zfliu@pku.edu.cn (Z.L.)

⁴ Key Laboratory of Advanced Carbon Materials and Wearable Energy Technologies of Jiangsu Province, Soochow University, Suzhou 215006, China

⁵ Center for Nanochemistry, Beijing Science and Engineering Centre for Nanocarbons, Beijing National Laboratory for Molecular Sciences, College of Chemistry and Molecular Engineering, Peking University, Beijing 100871, China

* Correspondence: r.g.mendes@ifw-dresden.de (R.G.M.); mhr1967@yahoo.com (M.H.R.)

Received: 30 October 2018; Accepted: 28 November 2018; Published: 5 December 2018



Abstract: The various forms of carbon nanostructures are providing extraordinary new opportunities that can revolutionize the way gas sensors, electrochemical sensors and biosensors are engineered. The great potential of carbon nanostructures as a sensing platform is exciting due to their unique electrical and chemical properties, highly scalable, biocompatible and particularly interesting due to the almost infinite possibility of functionalization with a wide variety of inorganic nanostructured materials and biomolecules. This opens a whole new pallet of specificity into sensors that can be extremely sensitive, durable and that can be incorporated into the ongoing new generation of wearable technology. Within this context, carbon-based nanostructures are amongst the most promising structures to be incorporated in a multi-functional platform for sensing. The present review discusses the various 1D, 2D and 3D carbon nanostructure forms incorporated into different sensor types as well as the novel functionalization approaches that allow such multi-functionality.

Keywords: carbon nanostructures; graphene; carbon nanotubes; graphene foam; sensors

1. Introduction

Carbon can present itself in many different natural and artificial allotropes [1–4]. These structures pursue unique electronic, mechanical, physical and chemical properties [5–7], which allow applications in a number of fields, especially in materials science and molecular electronics [8]. A few years ago we reviewed these nanostructures and their potential use as a drug delivery and diagnostics platform [4]. Currently we explore these versatile structures as multi-functional platforms for sensing. To this end, we explore the one-dimensional (1D), two-dimensional (2D) and three-dimensional (3D) carbon nanostructures, represented by carbon nanotubes (CNTs), graphene and graphene foam, respectively illustrated in Figure 1.

Sensing is an important area in modern society, because the use of sensors is a widespread reality, for example in the gas emission control industry, household security, automotive emission control, environmental monitoring and health care diagnosis. Most investigations have focused on

detecting oxygen (O_2) [9,10], ozone (O_3) [11], carbon monoxide (CO) [12,13], carbon dioxide (CO_2) [14], ammonia (N_3) [15], sulfur dioxide (SO_2) [15] and hydrogen (H_2) [16,17]. Other organic gases such as ethanol [18], benzene [19], isopropanol [20], acetone [21,22] and methanol [23] have also called attention to be detected. Different biological electroactive species and other biomolecules as glucose [24,25], neurotransmitters [26], ascorbic acid [27,28], uric acid [29], hydrogen peroxide (H_2O_2) [30] among others are also of great interest to be monitored due to the need of diagnosis of diseases [31]. There is a high demand for sensors that have a high selectivity, sensitivity and reversibility as well as high scalability, low costs and compact sizes to be incorporated in wearable devices.

To achieve these properties, the active sensing spot must ideally pursue a high surface area/volume ratio to increase the probability of adsorption of molecules and increase the sensitivity. The selectivity of the sensor is mostly achieved by functionalization with specific molecules that have a high affinity to the analytes of interest. Carbon nanostructures pursue all the ideal properties such as high surface area and can be easily functionalized. Currently, their relative cheap and simple production steps as well as advanced manipulation methods of a wide variety of carbon nanostructures makes them perfect candidates to be used in different types of sensors.

A key attention to the realization of sensors in general is directed to the integration of the recognition elements with the electronic elements, which can be classified into many different types, such as amperometric sensors, electrochemical impedance sensors, luminescence sensors and photoelectrochemical sensors [32]. In this way, the detection of chemical and biological targets is done by measuring electrochemical changes of the electrode that interacts with the analyte [33]. This highlights that the construction of high performance sensor platforms must not only consider the material used in the sensing area, but also the electrode materials, which will determine how well the signal can be transduced, transmitted and amplified.

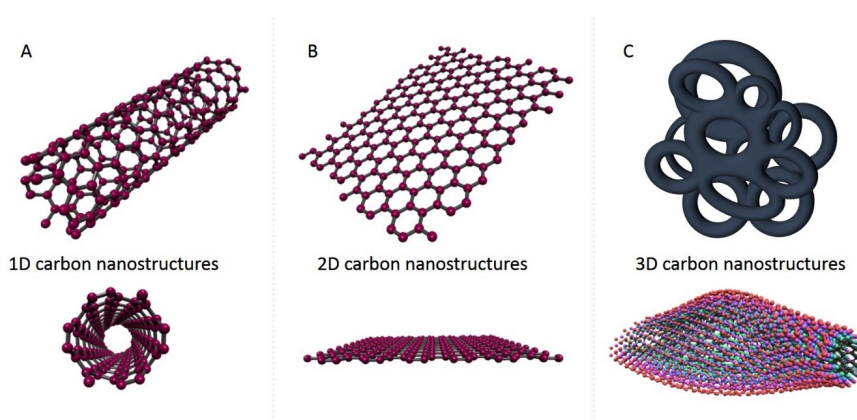


Figure 1. Illustration of the main carbon nanostructures described in this review. (A) 1D carbon nanostructures represented by carbon nanotubes. (B) 2D carbon nanostructures represented by graphene. (C) 3D carbon nanostructure represented by graphene foam, which is an intricate three-dimensional network of graphene.

The field of sensing using carbon nanostructures is very broad and diverse due to the variety of nanostructures and type of functionalization available. Therefore, most of the reviews in the field focus on a specific nanostructure with special attention to carbon nanotubes and graphene [34–37] or type of application [38]. More recently, research on 3D carbon nanostructures for a wide variety of applications has been rising and is mostly focused on synthesis approaches and battery applications [39–42] but to our knowledge this class of carbon nanostructures as sensors has not been covered in reviews. In this work we focus primarily on novel approaches used to build and functionalize carbon nanostructures as a multi-functional platform for sensing. Mostly of the presented strategies are applicable to a variety of gas, electrochemical and biosensors. This review is divided into 1D, 2D and 3D carbon nanostructures and subdivided into the various types of sensors where these nanostructures are

applied. The specific functionalization of each nanostructures and their state-of-the-art application is addressed. Finally, their future applications perspectives are briefly discussed.

2. 1D Carbon Nanostructures

It is almost twenty years since the discovery of CNTs by S. Iijima [43]. During these twenty years many papers related with CNTs unique properties [44] and applications were published. Nowadays CNTs even find their place in commercial applications, which is mostly in composite technology [45]. However, in the field of sensing devices, CNTs still have a wide field to be explored. Due to their very good electrical properties, possibility to functionalize their sp^2 backbone and large surface area (higher than graphite) [46,47], making them an interesting active material in sensing devices.

2.1. Carbon Nanotubes as Chemiresistors and Chemical Field-Effect Transistor

As mentioned previously, due to the good electrical properties of CNTs, they are a promising material to be used as a sensing layer in chemoresisting sensing devices. Chemoresistors are based on changing the electrical current flow through the material, which in the presence of a substance impacts the electron state of the active material. The first work related with CNT as a gas sensor is dated at the beginning of twenty first century. P. G. Collins et al. [48] researched the sensing ability of single-walled CNTs in the presence of oxygen. The experiment was carried out using a four-probe contact configuration at two temperatures 17 °C and 117 °C by flooding the device in cycles by air and evacuating it by vacuum pump. They also carried out alternative experiments by flooding the chamber with N_2 to confirm the sensor response to the oxygen molecules. Their research showed a rapid change in conductivity of the CNT-based active material. Moreover, CNT-based sensors were much faster than current ones based on metallic semiconducting devices, which work at high temperatures. The advantage of the device proposed by P. G. Collins et al. lies in the fact that it works at room temperature, which is also a milestone ahead in comparison to commercial ones using semiconducting active materials. Y. Wang et al. [49] presented chemiresistors based on single-walled CNTs to detect dimethyl methylphosphonate (DMMP) which is a flame retardant additive to polymer composites. The experiment was carried in a homemade chamber with N_2 as a carrier gas passing through a bubbler. The DMMP was evacuated after every test cycle. Their sensors were able to detect 5 ppm of DMMP in an experimental atmosphere.

L. Valentini et al. [50] researched the temperature influence on CNT-based chemiresistors in terms of changes in their resistivity. They concluded that the CNT structure is stable and able to go back to the starting state in the range between 25 and 250 °C. The resistivity of the CNT remains stable at 25 °C before heating. Above 250 °C structural changes can impact the material resistivity. They investigated their CNT-based chemiresistors affinity to NO_2 gas and they were able to detect the gas concentrations from 10 ppb and increased it stepwise to 100 ppb in temperature range from 25–250 °C. For the measurement carried out at 165 °C, a second thermal treatment increased the sensitivity of the sensor to NO_2 gas by almost 20 times, from approximately 3% to 56% after a second thermal treatment.

T. Ueda et al. [51] grew CNTs on a SiC surface and used them to prepare NO_2 and NO gas sensing devices. The detection level of CNT-based chemiresistors was 2 ppm. In this case they purified their device before the experiment by heating it to 80 °C in H_2O_2 in a heating bath to remove impurities and amorphous carbon. The experiment was carried out at room temperature for NO and at 100, 150 and 200 °C for NO_2 . They reported sensitivity of 2% for NO at room temperature and from 0.3% to 2.2% for NO_2 depending on the operating temperature. However, at temperatures lower than 200 °C the sensor was not able to return to the ground state. This is one of the reasons why different research groups use UV irradiation to promote a faster desorption of NO_2 gas molecules adsorbed at device surface (sensor recovery).

Nowadays there is a possibility to change the gas affinity to the active material in the sensor or its properties by functionalization, which tailors and improves the basic device properties like selectivity or detection range. CNTs are composed by sp^2 C=C bonds which take part in many

chemical reactions, especially in organic chemistry. Therefore, their chemical structure opens the possibility of functionalization. There are numerous papers reporting the functionalization of CNTs for instance by oxidation [52–54], thiolination [55–57] and bromination [58]. I. Sayago et al. [59] prepared chemiresistors from carboxylated CNTs and tested their sensing ability to NO_2 . Their chemiresistors showed high selectivity to NO_2 even when flushing it mixed with NH_3 . The sensor was still selectively active promoting the detection of NO_2 . Their work also highlighted the sensor performance when working in temperature higher than room temperature. At temperatures higher than $200\text{ }^\circ\text{C}$ the sensitivity achieved for 0.7 ppm of NO_2 was almost 3% higher in comparison to the sensor measured at $25\text{ }^\circ\text{C}$. M. Guo et al. [60] prepared thiolated CNTs by a number of chemical reactions from carboxylation to final thiolated CNTs. Their sensors have the ability to detect trace concentration of formaldehyde. H. Xie et al. [61] propose an amino-functionalized CNT system to detect formaldehyde gas. In their work they discuss the impact in resistivity due to changes of the sensor active material chemical structure. Their study shows clearly that the amino functionalization can improve the sensitivity to the analyte. In other words, unfunctionalized CNTs had marginal change in resistivity during exposure to formaldehyde, but after adding 5% of amino groups to the CNTs there was a clear change in resistivity of the active material when the gas sensor was exposed to formaldehyde concentrations of 20 and 200 ppb. D. Hines et al. [58] presented the response of brominated CNTs to eight different gaseous media. Chemiresistors based on brominated CNTs were reproducible and showed clear and noticeable response for concentrations under 1 ppm.

Another approach to sensing device production is using field effect transistors (FET). The working principle of these sensors is slightly different than in chemiresistors. FET devices consist of two electrodes: source and drain connected by a conducting material which is the charge carrier. Along with the conductive material there is another electrode separated from rest of the setup with a thin dielectric layer called the gate, to which the external voltage is connected. Gate voltage creates external electric field which has an impact in the resistivity/conductivity of sensor active material [62]. Figure 2 shows the schematics of chemiresistors and FET devices.

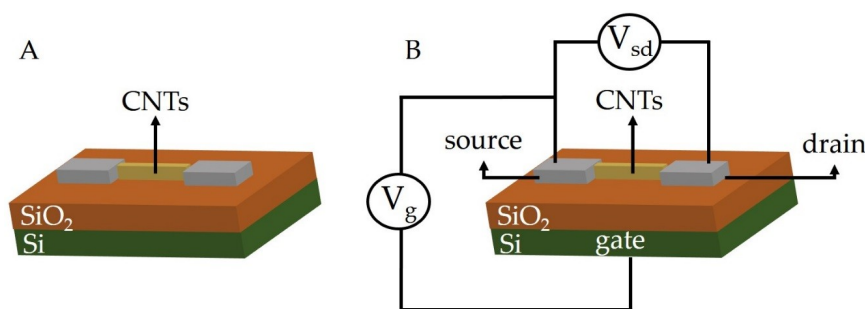


Figure 2. (A) Schematic chemiresistors and (B) ChemFET with carbon nanotubes as active material. V_g is the gate bias potential and V_{sd} is the source-drain potential.

The first FET device based on single-walled CNTs was presented by J. Kong et al. [63] to detect NO_2 and NH_3 . Metal oxide-based gas sensors exposed to NH_3 gas in concentration from 200 ppm to 1% usually have response time around 1 min. with relative sensitivity from 0.1 to 100 depending on the metal oxide used in the gas sensing experiment. The NH_3 sensor also showed efficiency at temperature higher than $350\text{ }^\circ\text{C}$. For NO_2 metal oxide-based gas sensors they also have quite fast response, which is approximately 1 min. In this case the relative selectivity was from 1 to 300 and, like in NH_3 case, they usually operate in temperatures from 250 to $600\text{ }^\circ\text{C}$ [64]. They also observed that their device has a rapid change in material conductivity and the response time vary from 0.5 min to 5 min. for NO_2 and 10 min. for NH_3 . The response time is related with the analyte concentration, what they clearly observe in NO_2 experiment. However, in comparison to the metal oxide devices, the biggest advantage of the J. Kong et al. sensor is the ability to work and be repeatable at room temperature. T. Someya et al. [18] prepared devices based on single-walled CNTs and investigated the

possibility to detect low concentrations of different alcohol vapors. The device was sensitive for a wide range of alcohol vapors and they highlighted the dependence of the sensor response relative to their vapors partial pressure value [18]. Figure 3 presents the change in drain current during exposure to various alcohol vapors.

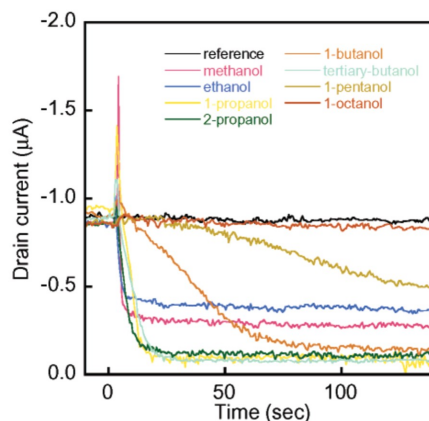


Figure 3. Drain current $V_{sd} = -100$ mV are shown as a function of time for application of saturated vapor of various kinds of alcohols: methanol, ethanol, 1-propanol, 2-propanol, 1-butanol, tertiary-butanol, 1-pentanol, and 1-octanol. Reproduced with permission from ref. [18].

Another interesting approach to apply CNTs to FET devices is presented by A. Star et al. methodology [65]. They decorated CNTs with several metals, mostly from D block of the periodic table, and exposed them to H_2 , NO_2 , NH_3 , H_2S and CO. They carried the sensing experiment at room temperature and in air with constant level of relative humidity. Figure 4 presents the sensor response for different gases of numerous metals used to decorate the CNT surface. The results were normalized so that 0.0 (blue color) means no response for the tested media and 1.0 (red color) is highest sensor response obtained. Their research highlighted the importance of nanomaterial functionalization to change their properties.

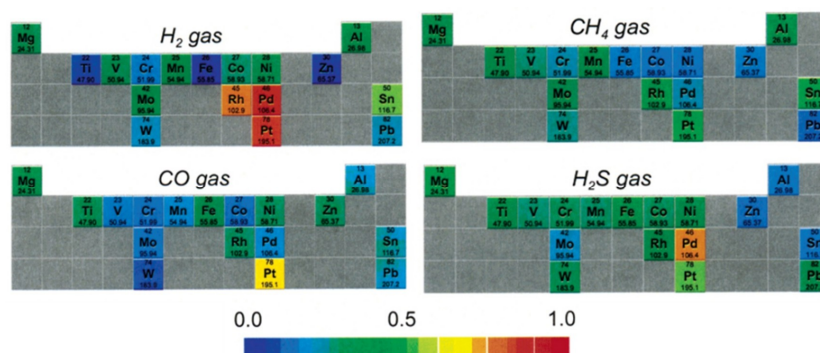


Figure 4. Correlation coefficients relating the conductance of devices decorated via metal evaporation with the gas profile of the tested gases, from 0 (no response) to 1 (maximal response). The catalytic metals were evaporated on carbon nanotube devices and tested for H_2 , CO, CH_4 , and H_2S gases as highlighted in the Periodic Table. Reproduced with permission from ref. [65].

J. P. Novak et al. [66], similarly to Y. Wang et al. [49], worked on a device that was able to detect DMMP, but J. P. Novak et al. used FET setup to detect DMMP by applying a positive gate bias to fully desorb DMMP from the CNT surface instead of exposing it to UV radiation or heating inside an oven. Their work also brings a very interesting idea to improve the selectivity between target gas/vapor and contaminants present in air like fuel vapors or humidity. They used special filters (built from glass wool and hydrogen-bonding acidic polycarbosilane called HC) to shield the sensor from the

influence of impurities. The ChemFET device was able to detect DMMP in the ppb range with high response and gate voltage assisted recovery has promising perspective in future applications [66]. Also, in comparison to Y. Wang group chemiresistor [49], J. P. Novak et al. FET sensor was able to detect lower concentrations of DMMP.

2.2. Carbon Nanotubes as Biosensors

There is a growing interest in the biochemistry of the human body as well as a growing need to increase the sensitivity and selectivity of sensor devices used in medicine. In most cases CNTs biosensors are based on CNT functionalized by covalent or non-covalent bond. The setup needed for that kind of measurement is slightly different than for the previously mentioned devices. CNT-based biosensors mostly use electrochemical techniques like amperometry, voltamperometry, chronoamperometry as a base for their research. Recently there are numerous works related with biosensing devices, report of multiple systems for detecting glucose, proteins or neurotransmitters like dopamine or serotonin.

Y. Lin et al. [67] worked on CNT-based glucose biosensors functionalized with GOx (glucose oxidase) enzyme at the tip of the nanotubes. The sensor was used in amperometric measurement and tested for the detection ability of glucose with detection limits at level of 0.08 mM and signal to noise ratio equal 3. Further work by numerous groups related with glucose detection was based on different CNT functionalization, but most of them had common feature which was partially functionalized CNT with glucose oxidase enzyme. Another very common way to improve selectivity in CNT-based sensors is preparing quasi composite of Naftion and CNTs, for instance in the works of X. Liu et al. [68], Y. L. Yao et al. [69] and K. Zhao et al. [70]. The purpose of Naftion addition is to decrease the negative impact of ascorbic acid which is one of the products of glucose metabolism in organism or uric acid which has an increased level and is related with diabetes.

Proteins are biopolymers that present in all organism from viruses to humans. The ability to detect low concentrations of protein can be helpful to find the cause or even cure for diabetes or HIV. One of the first work related with insulin sensor device was presented by J. Wang et al. [71] in which they prepared ruthenium oxide decorated CNTs as a coating to glassy carbon electrode. They achieve 1 nM detection limit. Over a decade later after, E. Martínez-Periñán with his group [72] presented an insulin sensor based on nickel (II) hydroxide CNT system with detection limits in the range of μM with confirmed stability (initial loss of the response was 10%) during multiple hours of continuous work [72].

Dopamine and serotonin are one of the most important neurotransmitters in the human organism. Their lowered level is related with many diseases, for instance with depression or other psychological disorders. The ability of detecting these two neurotransmitters at low concentrations is important from the medical point of view. Neurotransmitter biosensors research lies primordially on modified CNTs and on amperometric measurements method. B. E. K. Swamy et al. [73] prepared electrodes coated with oxidized CNTs and Naftion to detect simultaneously serotonin and dopamine. Their biosensor limit of detection for both neurotransmitters was lower than 300 nM. Y. Sun et al. [74] prepared multi-walled CNTs ionic liquid composite to realize similar experiment as above described. They prepared devices with high selectivity, sensitivity for both analytes with limit of detection under 100 nM.

3. 2D Carbon Nanostructures

A. K. Geim and K. S. Novoselov kickstarted the research and development related with 2D carbon materials by presenting graphene obtained by Scotch-Tape method in 2004 [75]. Briefly, 2D carbon materials are referred as crystalline structures with a honeycomb lattice and thickness of a single to few carbon atoms [76]. In the 2D carbon nanomaterials family it is possible to distinguish single and few layer graphene layers with very good thermal and electrical conductivity, large surface area (larger than the CNT case) [77]. Another very important member of the 2D carbon

nanomaterials family is the graphene oxide and its derivatives based on chemical functionalization, with most prominent representative in the form of reduced graphene oxide. Briefly, the graphene oxide pursue a quasi-graphene structure consisting mostly of an aromatic sp^2 backbone with the presence of oxygen containing functional groups like carboxyl, carbonyl and hydroxyl groups [78,79]. The presence of functional groups and other defects in the sp^2 structure have a direct impact onto the material properties, which leads to a decrease in conductivity and other properties in comparison to graphene [80,81]. To improve the electrical properties of GO-based materials it is usually applied chemical or thermal reduction to the starting material [81]. One of the biggest advantages of using graphene oxide in sensing applications is increased affinity of graphene oxide-based material to analyte substances due to the presence of functional groups and much bigger reactivity of the material, facilitating further functionalization. This can lead to precise tailoring of properties on demand. Herein, we will briefly refer application of 2D carbon nanomaterials as a sensor device.

3.1. 2D Nanomaterials as Chemiresistors and ChemFET

G. Ko et al. [82] prepared chemiresistors based on multi-layered graphene for NO_2 detection working at room temperature but with UV light-supported recovery of the sensor. Their sensor presented fast response and selectivity between NO_2 and air. They obtained almost 10% of sensitivity for 100 ppm of NO_2 . R. Pearce et al. [83] reported the shielding mechanism of multiple layers of graphene in the case of their chemi-resistive response, because single layer graphene has over 55,000 higher response to gas concentration in comparison its multilayer counterpart at 25 °C for one hour exposure to 2.5 ppm of NO_2 . Figure 5 presents the responses of single (left) and multilayer graphene (right) to different concentrations of NO_2 .

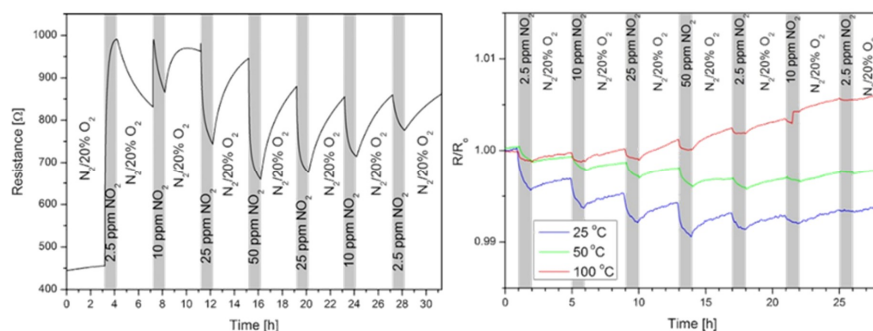


Figure 5. Left panel present response of single layer graphene exposed different concentrations of NO_2 . Right panel present response of multilayer graphene exposed to different concentrations of NO_2 tested in different temperature. Reproduced with permission from ref. [83].

F. Yavari et al. [84] also presented a graphene-based gas sensor for NO_2 and NH_3 detection. Their device operated at room temperature and atmospheric pressure. The sensor was exposed to concentrations from 0.1 to 200 ppm in the case of NO_2 and from 0.5 to 1000 ppm in the case of NH_3 . They also stated that in comparison to other types of materials like conductive polymers [85] or metal oxide [64] their device performance is impressive. They achieved around 19% higher sensor response for 200 ppm exposure to NO_2 than for polypyrrole sensor exposed to 1000 ppm.

Another interesting approach to graphene-based NO_2 gas sensor was proposed by H. Choi et al. [86]. Their sensor is based on a multilayer graphene grown using CVD and transferred to flexible polyimide surface with Au interdigitated electrodes. They investigated the sensor response in “flat” state for NO_2 diluted in N_2 . The gas mixture concentration was from 0.2 ppm to 5 ppm. They also researched the influence of device bending to sensor response. The gas sensor was exposed to 1 ppm NO_2 for 3 min. There was no decrease in signal when compared between flat and bend state. All measurements were carried out at room temperature. However, similar to the previously mentioned CNTs- and graphene-based devices, the desorption of gas molecules was very slow and the

sensor did not come back to ground state spontaneously. Therefore, they used external heating as a sensor recovery method.

H. J. Yoon et al. [87] proposed a device based on a few layer (~4 layers) graphene obtained by mechanical cleavage, which was firstly exposed to CO₂. They obtained promising results with quite fast responses and recovery time under 10 s. Their device was tested in three temperature values: 22, 40 and 60 °C. In all three cases they obtained a large increase in relative conductance over 20%. The results suggest that this sensor architecture has a great application potential in environmental monitoring systems.

K. R. Nemade et al. [88] proposed a device based on few-layer graphene (~6 layers) obtained by electrochemical exfoliation. Their chemiresistor sensor was exposed to CO₂ and the commercial mixture of propane and butane (LPG). They also assess the influence of temperature on the performance of the gas sensor for all the tested substances. They carried out the experiment at CO₂ concentrations from 30 to 50 ppm in a temperature range from 46 to 206 °C. For all chosen concentrations they estimated that the optimal temperature of operation for CO₂ gas sensor was 150 °C. They used the same protocol in the case of LPG and got the highest sensor response at 125 °C. The device showed almost perfect stability for constant exposure to 100 ppm solutions of both analytes for 30 days exposure. Their few-layer graphene-based sensor was also able to operate at room temperature condition, but the sensor response was quite low (under 1%) in both cases.

The first graphene-based FET gas sensor was proposed by F. Schedin et al. [89]. They prepared a FET sensor based on a single layer graphene obtained by micromechanical cleavage of graphite. The experiment was carried out in an evacuated glass container and filled in with analyte (NO₂ or NH₃ or CO or H₂O) diluted to 1 ppm concentration with inert gas (either nitrogen or helium). The device presented rapid response for NO₂, NH₃, CO and H₂O with limits of detection in the order of 1 ppb. However, after removing the detected gas from the chamber, the sensor still presented stable signal of response. They concluded that the adsorption of gas molecules at room temperature on the graphene surface is stable. The F. Schedin team used annealing at 150 °C under vacuum to fully recover the sensing ability of the device.

M. Guatam et al. [90] prepared a graphene-based FET sensor for detecting NH₃. They carried out an experiment in range of temperatures from 27 to 100 °C in dry air and continued vacuum. They observed that with the temperature increase, the sensing response of devices grow linearly. They also reported general problems with the sensor recovery only for the dry air flow experiment. Therefore, they proposed other ways in which the air flow is combined with infra-red irradiation or dry air flow combined with vacuum annealing.

As mentioned earlier, one of the biggest advantages of functionalized graphene-based materials (graphene oxide, reduced graphene oxide, functionalized graphene oxide) in comparison to pristine graphene is the increased affinity to detect molecules due to the presence of sp² structural defects (e.g., presence of functional groups). That is why these types of 2D materials are more promising in gas sensing applications.

In the case of graphene oxide (GO) there is a small amount of reports on chemiresistors and FET devices due to its more insulating than conductive properties [81]. That fact was noticed and highlighted by S. Prezioso et al. [91]. They prepared a device by drop casting GO material onto platinum interdigitated structure, and carried humidity sensing experiment for GO and annealed GO at 200 °C in ultra-high vacuum. The goal of that research was to study the effect of the chemical composition of the material during experiment in higher experimental temperature. They chose two ranges: from 25 to 150 °C and from 25 to 200 °C. The experiments were performed in a dry air atmosphere. They concluded that the chemical composition of the material has a clear impact onto the baseline conductivity and desorption time, which was faster for the annealed GO. They also tested the GO-based sensor for detecting low concentrations of NO₂. Their device was able to detect NO₂ at concentrations on the ppb level at 150 °C.

A. P. Taylor et al. [92] proposed an electro-sprayed GO chemiresistive detector with a four point electrodes connection and compared its performance with commercial humidity detectors (Honeywell HIH-4000). They carried out two types of experiments. The first part was based on quick change of relative humidity value to check if the GO-based sensor was able to detect dynamic relative humidity changes. It turns out that the GO-based sensor was able to surpass the response of the commercial one. This suggests that GO-based humidity sensors are able to track changes in relative humidity continuously. The second part of experiments demonstrated that the conductivity change of the material is in linear relation with the percentage value of relative humidity.

Our group [93] works on the impact of functionalization to investigate the detecting ability of GO in comparison to reduced and functionalized GO with thiol groups. Our goal was to prepare a gas sensing device operating fully at room conditions (e.g., room temperature and atmospheric pressure) without any external recovery promotion mechanism like the ones mentioned before such as heating or UV irradiation. It was also our aim to highlight the impact of the chemical composition of the active material in relationship to the device behavior exposed to chosen analytes, namely NO₂ and ethanol. The experiments were carried out by flushing the sensor in 5-minutes-cycles of exposure to NO₂ or ethanol diluted in nitrogen to concentrations from 100 to 300 ppm. Prior to the measurement the chamber was flushed for 15 min with inert gas, in this case nitrogen. We observed different behaviors of the device exposed to analytes in the case of GO sensors, reduced GO and partially reduced thiolinated GO. Every sensor type had different responses, recovery time and relative sensor response in comparison to each other. We also studied the reproducibility and stability of the sensor. This was performed by measuring at least four cycles for a certain concentration and repeated the measurement conditions a few days later. The sensors prepared from GO and GO-based materials have stable and reproducible response with marginal changes in the signal shape, response time, recovery time, and amplitude.

There are many more reported works related with reduced GO as a gas sensor. J. D. Fowler et al. [94] proposed chemiresistors based on hydrazine reduced GO for the detection of NO₂, NH₃, and 2,4-dinitrotoluene (DNT). They carried out experiments at room temperature with 10 min sensor exposure to analyte followed by 10 min. purging in dry nitrogen. They observed a clear change in sensor resistivity for all three analytes: 13% for NO₂, 2.5% for NH₃ and 0.03% for DNT, with limit of detection in case of DNT equals to 28 ppb. Their result for NO₂ and NH₃ was similar to the one proposed by F. Schedin et al. [89] done with micromechanical cleavage graphene. They also carried out detection of 5 ppm NO₂ on micro hotplate and concluded that, as in the previous cases, the analyte desorption from sensor surface is promoted by heating (sensor recovery is faster) but at the expense of loss in sensitivity. G. Lu et al. [95] prepared thermal reduced GO for NO₂ detection. In their case, the GO was prepared by Hummers method and was thermally reduced by annealing in argon atmosphere for 1 h. They conducted the experiments in various concentrations and reported a linear dependence between concentration and relative response percentages. They obtained similar results in the case of sensor response percentages in comparison to F. Schedin et al. [89] graphene device and J. D. Fowler et al. [94] hydrazine reduced GO.

G. Lu et al. [96] prepared back-gated FET sensor for detecting NO₂ and NH₃ based on GO reduced by hydrazine. Their device showed a superior performance of the FET device when compared to the chemiresistors reported previously in reference [95]. The switching of sensor architecture from chemiresistors to FET device improved sensor response from ~2.5% for the chemiresistors to almost 10% for the FET device, which is 4 times better than the chemiresistor device. In the case of NH₃ they also noticed an improvement of performance. A chemiresistor reported by G. Lu et al. [97] had 0.4 lower response in resistivity during exposure to 1% solution of NH₃ in relation to reduced GO-based FET device reported in reference [96].

V. Dua et al. [98] incorporated in their research two novel approaches in reduced GO-based gas sensors. In the first, they used ascorbic acid (Vitamin C) for an environmentally friendly reduction of GO for gas sensing applications. The authors reported that their Vitamin C reduced GO layer have a similar conductivity to previously reported hydrazine reduced GO. Due to the toxic and

explosive nature of hydrazine, applying a new environmentally friendly reducing agent in gas sensing applications is definitely an advantage. Another unique approach was presented by preparing a flexible device by printing the active material layer onto a polymer surface. Such flexible sensors showed response to NO_2 , NH_3 , Cl_2 , methanol, ethanol, toluene and dichloromethane. Figure 6 presents example response plots and the sensor selectivity diagram. The sensors operated in a special chamber in which they were exposed to an analyte. The recovery process was quite slow (approximately 2 h) under vacuum. External UV irradiation was used to promote desorption and the time needed for the sensor to get back to the ground state was under 5 min.

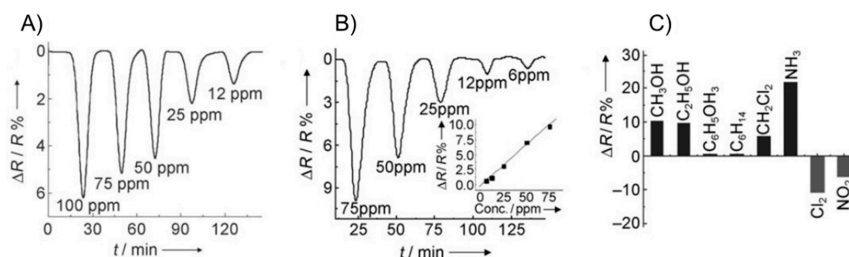


Figure 6. Example vapors sensing characterization of RGO/Inject-Printed chemiresistors. (A) Response vs time plot of sensor response exposed to NO_2 . (B) Response vs time plot of sensor response exposed to Cl_2 . (C) Summary of sensor response for different measured media. Reproduced with permission from ref. [98].

One of the newest approaches to flexible gas sensors was proposed by H. J. Park et al. [99]. They prepared electrospun fabric from nylon-6, coated it with GO and reduced it with a solution of iodine acid and acetic acid. Their device showed slightly better (approximately 0.5 higher) sensor relative response for 1 ppm of NO_2 than in the work presented by V. Dua et al. [98]. They also showed the ability of detecting low concentrations of NO_2 (1 ppm) in the bent state. However, the device response in the bent state was 2 times lower than in the flat state.

A. Lipatov et al. [100] also studied the ability of thermally reduced GO to detect different alcohol vapors. They tested the response for methanol, ethanol, isopropanol and water vapor. For all analytes they obtained a clear stable response of the device with small differences in response behavior depending on the analyte type. This opens up new possibilities for further research on improving the selectivity of these analytes. Their sensor device did not use external heating or UV irradiation to promote desorption of analyte molecules from the sensor surface.

W. Yuan et al. [101] and A. Zöpfl et al. [102] pushed the research forward regarding the impact of functionalization onto GO- and reduced GO-based devices and their selectivity. W. Yuan team used hydrazine as a reducing agent, ethylene diamine (EDA) as both a partial reducing and chemical composition modification agent. Aryl diazonium salt was used to introduce sulfur to the chemical composition of GO. After these 3 types of functionalization, they compared the impact of the introduced functional groups onto the sensing ability of device exposed to various concentrations of NO_2 . They compared the response signal obtained for reduced, sulfonated and EDA-functionalized graphene-based materials in presence of 50 ppm of NO_2 . Sulfonated and EDA-functionalized materials exhibited respectively 16- and 4-times higher responses than reduced GO.

A. Zöpfl team compared reduced GO, octadecylamine (ODA)-functionalized and reduced GO-based nanocomposites decorated with metal oxides (TiO_2 , MnO_2) and metal nanoparticles (platinum and palladium). They tested the behavior of chemiresistors for exposures to different concentrations of NO_2 , H_2 , CH_4 and compared the results between the chosen functionalization materials (for instance, Pd functionalization increased the relative response of gas sensor for hydrogen from 0.1 to 0.6 in comparison to other devices). Their results confirm that functionalized GO is a promising material to tailor the selectivity of the gas sensor.

3.2. 2D Carbon Nanomaterials as Biosensors

One of the first reports on graphene-based glucose sensor was done by C. Shan et al. [103]. The core architecture of their device was based on a nanocomposite electrode consisting of graphene and polyethyleneamine-functionalized ionic liquid. They conducted cyclic voltamperometry measurement with different scan rates. They obtained electrodes with good linear responses for 2 to 14 mM of glucose concentration. The prepared electrode was stable with minimal changes in response and the current did not go over the 5% error barrier over 1 week from the initial measurement. H. Wu et al. [104] reported bionanocomposite films consisting of glucose oxidase, platinum, chitosan and thermally expanded GO to partially reduced GO. Their composite had good sensitivity for glucose with theoretical detection limit of 0.6 μ M. They attributed the results of their cyclic voltamperometry detection experiment to the large surface area of graphene and good electron transfer between partially reduced GO and platinum.

D. H. Shin et al. [105] decorated graphene grown in CVD with electrodeposited palladium in the presence of different sulfuric acid concentration in the electrolyte, which led to the formation of particles with different morphologies as shown in Figure 7. They used these structures to prepare a FET glucose sensor.

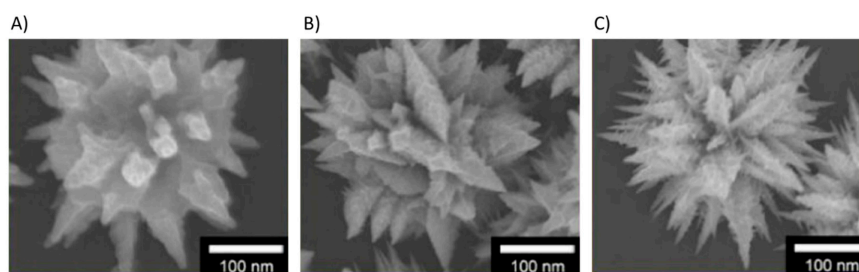


Figure 7. SEM images of electrodeposited palladium structure with various sulfuric acid concentrations (A) 1M, (B) 0.1M, (C) 0.01M. Reproduced with permission from ref. [105].

They obtained a device with good response and detection limit of 1 nM glucose, which was lower than in, for instance, CNT-based devices reported by L. Meng et al. [106]. However, the FET sensor based only on Pd/Graphene structure was not selective in the presence of uric acid and ascorbic acid. For this reason, the Shinc group prepared a device with glucose oxide and a Naftion coating. After these modifications the FET sensor was selective for glucose in presence of uric and ascorbic acid.

S. Lin et al. [107] prepared a flexible electrochemical glucose detector with active material consisting of laser-scribed graphene (LSG-laser reduced GO), chemically reduced GO and laser-scribed graphene coated with copper nanoparticles. The LSG/Cu electrochemical flexible electrode performance dropped only by 10% when stored in ambient conditions for 30 days. The sensor limit of detection was 0.35 μ M which was almost two times smaller than, for instance, the work presented by H. Wu et al. [104]. Their sensor was also selective to glucose in the presence of ascorbic and uric acid without the need of a Naftion coating.

X. Xuan et al. [108] proposed a wearable flexible glucose detector based on reduced GO decorated with platinum and gold nanoparticles in the form of a wristband. Apart from the standard glucose measurement reported earlier, Xuan's sensor exhibited good analytic activity with response time of 12 s. They also investigated the ability of glucose detection in sweat. The collected human sweat from healthy and diabetic patients. They also prepared glucose solutions in human sweat. The sensor was able to detect 0.1 mM of glucose in sweat, which is a huge success towards the application of that type of device in current and future health care programs.

G. Xu et al. [109] prepared a laser-scribed graphene-based electrochemical dopamine sensor coated with poly(3,4-ethylenedioxythiophene) (PEDOT) layer. They used cyclic voltammetry and differential pulse voltammetry with nitrogen purging to remove oxygen from the measurement setup. They carried out measurements in phosphate-buffered saline (PBS) electrolyte solution at two pH values, namely 7.0 and 7.4 in the presence of uric and ascorbic acid. They also tested the influence of

a PEDOT layer on dopamine detection. It came out that pure graphene electrodes have low affinity and selectivity towards dopamine in presence of ascorbic and uric acid. However, the PEDOT layer drastically increased the current flow in the presence of dopamine. They achieved simultaneous detection of dopamine in the presence of ascorbic and uric acid with high selectivity, sensitivity of $0.22 \pm 0.01 \mu\text{A}/\mu\text{M}$ and a low detection limit of $0.33 \mu\text{M}$.

In the case of other biomolecules there were reports on graphene-based sensors detecting *E. coli* bacteria. A. Pandey et al. [110] prepared a capacity/impedance sensor based on graphene nanoplates and monolayer graphene with a gold electrode interdigitated array. The graphene surface was activated by a PASE linker for further *E. coli* antibody functionalization. Both devices showed reaction in the presence of *E. coli* O156L:H7 bacteria. The sensitivity of the developed sensor was 4 pF for graphene nanoplates sensor and 1 pF for monolayer defect-free graphene per unit change in analyte concentrations of 10–100 CFU/mL. However, the monolayer graphene-based device had 10 times better sensitivity in comparison to nanoplates-based device, which contained 100 CFU/mL. Both devices are promising setups for application in the detection of pathogenic *E. coli* bacteria.

B. Thakur et al. [111] proposed reduced GO-based FET device covered with gold nanoparticles to anchor *E. coli* antibodies. The FET device demonstrated rapid response with limits of detection at concentration of 103 CFU/mL. The authors reported that this limit of detection is lower than in cases of some commercial *E. coli* detectors. The FET device gave a stable and reproducible signal for 3 measurements. They also reported that there is a possibility of recovery of this type of device by using suitable regeneration buffers. R. Singh et al. [112] recently showed that reduced GO has been integrated in a microfluidic chip to create a reduced GO-based electrochemical immunosensor for the label-free detection of the H1N1 influenza virus. This was done by covalently bonding the NH_2 end of monoclonal antibodies specific to virus with carboxyl end reduced GO. The sensor showed a linear detection behavior in the range of 1 to 10^4 PFU/mL.

4. 3D Carbon Nanostructures

The appearance and rise of two-dimensional carbon nanostructures triggered also the desire to explore the possibility of creating their three-dimensional structures counterparts in order to exploit their thermal and electrical properties for innumerable applications [113]. The realization of three-dimensional structures based on graphene also known by graphene foam was theoretically demonstrated [114] and successfully produced using reduced graphene oxide as well as grown using CVD [115–120]. Such 3D structures change its resistance when perturbed locally, which can serve to sense local changes, for example in temperature and electromagnetic field. These properties rendered studies to investigate pure and functionalized graphene foam as different types of sensors [121–123].

4.1. 3D Carbon Nanostructures as Chemical and Electrochemical Sensors

F. Yavari et al. [124] reported the use of a unfunctionalized and flexible 3D graphene foam, which can be used for sensing NO_2 and NH_3 with high sensitivity and reversibility. The graphene foam was synthesized using a scaffold of porous nickel as a template for the deposition and growth of graphene with CVD with a posterior removal of the nickel template, remaining only the three dimensional network of graphene [115]. The charge carriers can move rapidly with small resistance, which results in high electrical conductivity. Trace amounts of NO_2 and NH_3 adsorbed on graphene cause changes in the conductivity of the graphene foam and can be detected. The high porosity of the graphene foam increases the surface area and it facilitates for the homogenous distribution of the investigated gases. It is also important to mention that the whole process is reversible and applied in environmental monitoring and gas detection against terrorism.

The resistance of unmodified 3D graphene structures was also used to detect other organic molecules, among which are chloroform, ether and acetone as demonstrated by H. Hua et al. [125]. The graphene foam was also synthesized using a nickel scaffold as a template while the resistance curves for the various molecules were acquired and an algorithm was applied to discriminate the

specific molecules with over 97% accuracy. The results show the promising ability of graphene foam to detect a wide spectrum of molecules combined with algorithms to identify specific compounds or contaminants. A sketch of the graphene foam sensor architecture is shown in Figure 8.

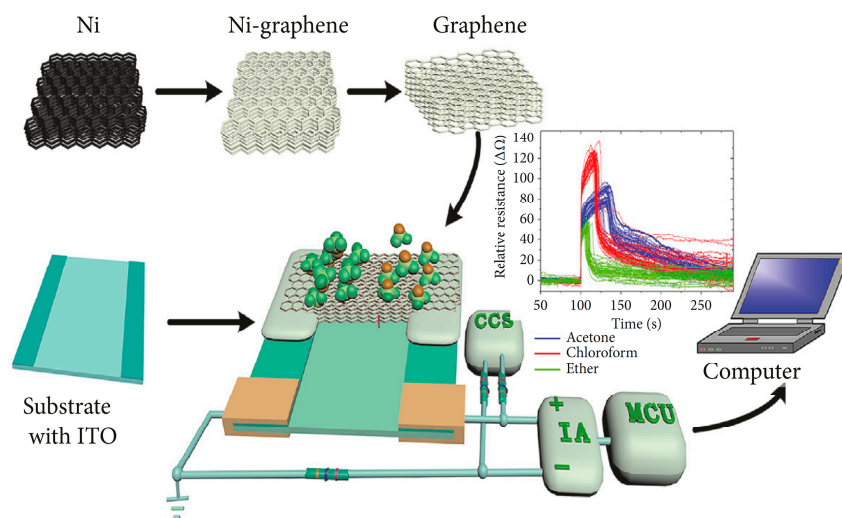


Figure 8. The fabrication process of 3D graphene foam and the electrical resistance time domain detection system (CCS: constant current source; IA: instrument amplifier; MCU: micro control unit). Reprinted with permission from ref. [125].

The unique structure of 3D graphene foam for sensors has also been demonstrated for functionalized or hybrid graphene foam architectures [121]. It is known that cobalt oxide (Co_3O_4) is a promising functional material for electrochemical [126] and gas sensors [127–129]. L. Li et al. [130] used flower-like Co_3O_4 nanostructures supported on 3D graphene foam as a platform for sensing ethanol vapor with a concentration as low as 15 ppm at 320 °C. A similar functionalization approach was achieved by Y. Ma et al. [131]. In their work they demonstrated the synthesis of graphene foam functionalized with $\alpha\text{-Fe}_2\text{O}_3$ to build an electrode-like sensor with the ability to detect and quantify the presence of nitrite. The detection of nitrite was validated in various water sources by anodic stripping voltammetry analysis and the electrochemical impedance spectrum.

4.2. 3D Carbon Nanostructures Biosensors

Decorated 3D graphene foam has also been demonstrated to be suitable for biosensors to detect a wide variety of biomolecules [132,133]. The use of 3D graphene foam functionalized with Co_3O_4 nanowires has been shown as an excellent enzyme-free electrochemical glucose detector. X.-C. Dong et al. [134] used this 3D graphene/ Co_3O_4 composites to sense the presence of glucose in an extreme low concentration (<25 nM). The use of enzymes to detect glucose using a nitrogen-doped CNT-functionalized 3D graphene foam was demonstrated by P. Fan et al. [135] as shown in Figure 9. This was achieved by immobilizing glucose oxidase on nitrogen-doped CNT-functionalized 3D graphene foam composite and measuring changes in the conductivity of the system in the presence of glucose in a linear range from 0.05 to 15.55 nM. The detection of glucose using graphene foam decorated with nickel nanoparticles was also demonstrated by L. Wang et al. [136]. The linear range of their electrochemical sensor was from 15.84 μM to 6.48 mM with a detection limit reaching 4.8 μM .

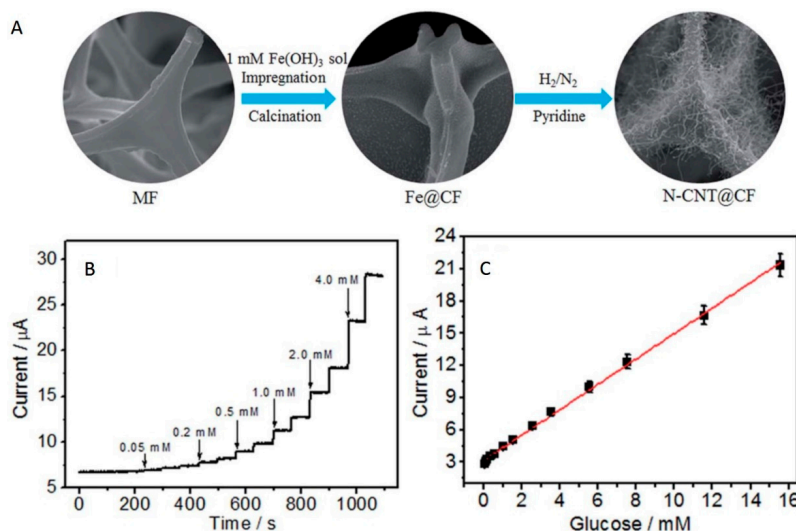


Figure 9. (A) Schematic illustration for the preparation of nitrogen-doped CNT@3D graphene foam. (B) Current-time curve of glucose oxidase on nitrogen-doped CNT@3D graphene foam for different concentrations of glucose in stirred 0.1 M O₂-saturated PBS (pH 7.0) at -0.45 V. (C) Calibration curve of the glucose oxidase on nitrogen-doped CNT@3D graphene foam for glucose. Reproduced with permission from ref. [135].

Similarly to Co₃O₄, manganese oxide (Mn₃O₄) was also used to decorate 3D graphene foam to detect glucose non-enzymatically as well as hydrogen peroxide (H₂O₂) as shown by P. Si et al. [137]. The Mn₃O₄ is found on the graphene walls in form of nanoflakes. The high surface area of the Mn₃O₄@3D graphene foam has a large surface area, providing abundant active sites for electrocatalytic reactions and electron transport. Cyclic voltammetry was used to study the electrochemical changes in the oxidation/reduction of Mn₃O₄ in the presence of glucose and H₂O₂. The selectivity of the biosensor was demonstrated by negligible current responses to the addition of 0.1 mM uric acid, ascorbic acid and acetaminophen, which are common electroactive species in the blood.

The detection of H₂O₂ was accomplished using hybrid composites containing 3D graphene foam with high sensitivity. For example, J. Liu et al. [138] functionalized the graphene surface of the whole 3D structure with a complex composite of horseradish peroxidase, methylene blue and CNTs, rendering excellent performance to detect H₂O₂ with a low concentration (58 nM) and a fast response. C.-C. Kung et al. [139] incorporated platinum/ruthenium (PtRu) bimetallic nanoparticles on the porous structure of the graphene foam and reached a detection limit of 0.04 μ M for H₂O₂ also with minimum influence of other electroactive species.

Since copper oxide (CuO) has shown promising results to catalyze biomolecules [140,141], Y. Ma et al. [142] decorated graphene foam with CuO nano-flowers to construct a sensor with high sensitivity for ascorbic acid (vitamin C). The sensing of ascorbic acid was done by measuring the resistance and changes in the current passing through the decorated graphene foam in the presence of ascorbic acid and a calibrating solution of phosphate buffer solution (PBS). The detection of the important neurotransmitter dopamine was also achieved using 3D graphene foam by X. Dong et al. [143]. Their work showed that hydrophobic and π - π interactions between the dopamine and the graphene walls cause measurable changes in the conductivity of the 3D graphene foam, allowing the detection of dopamine at concentrations as low as 25 nM.

H. Yan Yue et al. [144] used zinc oxide (ZnO) nanowires to functionalize graphene foam to selectively detect uric acid, ascorbic acid and dopamine by differential pulse voltammetry. They claim that uric acid is of especial attention since it can be used as a biomarker for Parkinson's disease. Patients with Parkinson's disease have levels of uric acid 25% lower than in healthy individuals. These molecules coexist in many biological systems, therefore sensors with high sensitivity and selectivity are crucial. Their functionalized 3D graphene foam sensor was able to detect these molecules

without any cross interference with a limit of detection of 0.5, 0.5 and 5 μM for uric acid, dopamine and ascorbic acid, respectively.

4.3. Other Sensors Based on 3D Carbon Nanostructures

There is a class of sensors based on 3D carbon nanostructures used to measure strain. These sensors are mostly based on the incorporation of polymers to the porous architecture of the graphene foam to produce a flexible and stretchable sensor. For example, Y. A. Samad et al. [123] embedded a graphene foam into a polydimethylsiloxane (PDMS) to create a pressure/strain sensor that can measure the human blood pressure and heartbeat.

In order to increase the bending sensitivity of the 3D graphene foam/PDMS composite, R. Xu et al. [145] introduced a thin layer of polyethyleneterephthalate (PET) in one of the sides of the 3D graphene foam/PDMS composite causing a variance in the electrical resistance of the composite when bended to the side with and without PET due to the different bending properties of the different sizes of the composite. Y. Qin et al. [146] demonstrated that the infusion of polyimide into a brittle reduced graphene aerogel rendered a superflexible three-dimensional architecture able to sense deformation caused by compression, bending, stretching and torsion with excellent durability as illustrated in Figure 10. Such graphene foam/PDMS composites were also demonstrated to have enormous application possibilities into biomechanical systems and wearable devices [147].

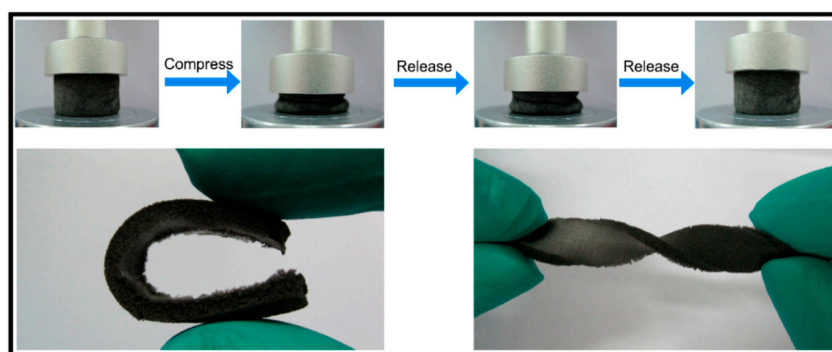


Figure 10. Images showing the recovery process of a compressed reduced graphene foam/polyimide composite and the high levels of bend and torsion deformations. Reproduced with permission from ref. [146].

Monolithic 3D graphene foam was also used as a precursor for graphene quantum dots, which were used for sensing iron ions (Fe^{3+}) as presented by A. Ananthanarayanan et al. [148]. Such graphene dot architecture could not be synthesized using the 2D graphene form, because the graphene film quickly disintegrates leading to a low yield of graphene quantum dots. The graphene quantum dots were produced by applying a voltage to the 3D graphene foam in a mixture of 1-Butyl-3-methylimidazolium hexafluorophosphate (BMIMPF₆) and acetonitrile (10% v/v) as an electrolyte. The resulting solution was centrifuged and the graphene quantum dots were collected. Gel electrophoresis suggests a narrow size distribution of the graphene quantum dots, which emit blue fluorescence under UV light of 365 nm. In the presence of Fe^{3+} ions there is a significant quenching (68% quenching in 400 μM of Fe^{3+}) whereas other ions such as Mg^{2+} , Fe^{2+} , Zn^{2+} , Co^{2+} , Ni^{2+} , Cd^{2+} and K^{+} were not able to show significant quenching of the graphene quantum dots.

5. Summary and Conclusions

In summary, we presented investigations that highlight the great versatility of 1D, 2D and 3D carbon nanostructures as an exceptional high sensitivity and specificity platform for sensing. Carbon nanostructures pursue a large surface area providing huge functionalization potential, which enables the design of sensors with high specificity depending on the type of functionalization.

The high sensitivity is related with the unique electrical properties of the various nanostructures. Unlike other materials purely based on metals or metal oxides, carbon nanostructures have a higher compatibility with polymers, which allows the formation of composites that not only present a better sensitivity, but also opens up the field of flexible electronics and allow the design of a wide range of wearables that can constantly monitor the surrounding conditions and health of individuals.

Although great progress has been achieved in the synthesis of various carbon nanostructures, large scale production remains a challenge, especially concerning the fabrication of material without defects and with reproducible properties. For example, the synthesis of graphene leads to the formation of grain boundaries and intrinsic point defects that influence the electrical properties of the material. Moreover the transfer processes of carbon nanostructures from the synthesis substrates to the actual device is complex and in many cases lead to the formation of defects that limit the reproducibility and scalability of sensors based on these materials. For example, the lack of precise defect control in graphene oxide-based sensor may lead to small differences between material batches, which can have huge impact in the sensing mechanism. In other words, there is still a lack in the synthesis control of the nanostructures, separating the design of carbon-based sensors from the commercial application of these devices.

Another general problem of sensors is related with the cross sensitivity. Nowadays it is still a challenge to create a device with a specificity capable of distinguishing between similar chemicals. Progress with carbon nanostructures has been achieved, as shown before [125]. In this sense, we envision that the innumerable possibilities of functionalization is the most promising approach to reach specificity and this tailoring of properties is achievable with carbon-based nanostructures. Moreover, we should not ignore the increasing development and refinement of softwares for data analysis as well as the emerging field of artificial intelligent, which may provide new insights in data analysis that will enable more detailed processing of the detected signal, minimizing the cross-sensitivity problem.

The investigations reviewed here suggest that carbon-based sensors are already a reality in the lab and a continuous investment in this field is essential to not only develop more accurate sensors but also incorporate these into wearable devices and in the routine of industrial and medical processes. Table 1 highlights and summarizes all the carbon nanostructures included in this review as well as their functionalization, molecule detected and the corresponding detection limit of the many different sensor architectures described in details within the main text.

Table 1. Carbon nanostructures used as sensors, their functionalization and corresponding analyte discussed within this review.

Carbon Nanostructure	Functionalization	Analyte (Detection Limit)	References
1D carbon nanostructure			
Multi-walled CNTs	Au nanoparticles	NO ₂ (0.1 ppm), CO (2 ppm), C ₆ H ₆ (-)	[9]
Multi-walled CNTs	COOH	O ₂ (0.3%)	[10]
Single-walled CNTs	FeOOH	O ₃ (4.1 ppb)	[11]
Single-walled CNTs	CuCl	CO (20 ppm)	[13]
Multi-walled CNTs	SnO ₂	ethanol (30 ppm), methanol (30 ppm), H ₂ S (9 ppm)	[14]
Multi-walled CNTs	maleic acid, acetylene	NH ₃ (10 ppm)	[15]
Multi-walled CNTs	Pt nanoparticles	H ₂ (4%)	[16]
Single-walled CNTs	Pd doping/sputtering	H ₂ (0.5%)	[17]
Single-walled CNTs	-	ethanol, methanol, 1-propanol, 2-propanol, 1-butanol, tertiary-butanol, 1-pentanol, 1-octanol (2 mmHg for all analytes)	[18]
Multi-walled CNTs	ethyl cellulose	benzene (2.5 ppm)	[19]
Single-walled CNTs	poly(vinylpyrrolidone)	isopropyl (100 ppm)	[20]
Single-walled CNTs	LaFeO ₃	methanol (1 ppm)	[23]
Multi-walled CNTs	-	dopamine (500 nM), glutamate (10 µM)	[26]
Multi-walled CNTs	Pt-Ni alloy	uric acid (0.03 µM)	[29]
Single-walled CNTs	-	O ₂ (1 × 10 ⁻¹⁰ torr)	[48]
Single-walled CNTs	3-aminopropyltrimethylsilane	dimethyl methylphosphonate (5 ppm)	[49]
Multi-walled CNTs	-	NO ₂ (10 ppb)	[39,40]
Single-walled CNTs	Br	ethanol (608 ppb), HCl (769 ppb), NH ₃ (1645 ppb), sulfuric acid (286 ppb)	[58]
Double- and Multi-walled CNTs	-	NO ₂ (0.1 ppm)	[59]
Multi-walled CNTs	thiol	formaldehyde (10 ppm)	[60]
Multi-walled CNTs	amine	formaldehyde (20 ppb)	[61]
Single-walled CNTs	Au, Pt, Pd, Rh	H ₂ (0.4%), CH ₄ (0.5%), CO (2%), H ₂ S (50 ppm)	[65]
Single-walled CNTs	-	dimethyl methylphosphonate (1 ppb)	[66]
Multi-walled CNTs	glucose oxidase	glucose (0.08 mM)	[67]
Single-walled carbon nanohorns	glucose oxidase, nafion	glucose (6 µM)	[68]
Multi-walled CNTs	horseradish peroxidase, glucose oxidase	glucose (0.5 µM)	[69]
Multi-walled CNTs	Pt nanoparticles	glucose (1 × 10 ⁻⁵ mol/L)	[70]
Single-walled CNTs	Nafion	dopamine (250 nM), serotonin (130 nM)	[73]
Multi-walled CNTs	1-butyl-3-methylimidazolium hexafluorophosphate	dopamine (60 nM), serotonin (8 nM)	[74]
Multi-walled CNTs	RuO _x	insulin (1 nM)	[71]
Multi-walled CNTs	Ni(OH) ₂ -Nafion	insulin (85 nM)	[72]
Single-walled CNTs	Pd nanoparticles	glucose (0.2 µM)	[106]

Table 1. Cont.

Carbon Nanostructure	Functionalization	Analyte (Detection Limit)	References
Single-layered graphene	SnO ₂	CO (30 ppm)	[12]
SiO ₂ -Graphite	CuO	glucose (0.02 mmol/L)	[25]
Single-layered graphene	-	NO ₂ (100 ppm; 2.5 ppm; 100 ppm), NH ₃ (500 ppb), CO ₂ (10 ppm)	[82–84,87,89,90]
Multi-layered graphene	-	CO ₂ (3 ppm), liquid petroleum gas (4 ppm)	[88]
Graphene oxide	COOH, OH	NO ₂ (20 ppb), NH ₃ (500 ppm), 2,4-dinitrotoluene (28 ppb)	[91,92,94,95]
Graphene oxide	ascorbic acid, thiol	ethanol (100 ppm), NO ₂ (100 ppm)	[93]
Reduced graphene oxide	-	NH ₃ (1%; 100 ppm), Cl ₂ (100 ppm), NO ₂ (100 ppm; 1 ppm), methanol (500 ppm), ethanol (500 ppm), isopropanol (500 ppm)	[96–100]
Reduced graphene oxide	sulfophenyl, ethylenediamine	NO ₂ (3.6 ppm)	[101]
Reduced graphene oxide	Octadecylamine, Pd- and Pt-doping, MnO ₂ and TiO ₂ nanoparticle	NO ₂ (25 ppm), CH ₄ (1000 ppm), H ₂ (500 ppm)	[102]
Multi-layered graphene	Poly(vinylpyrrolidone), glucose oxidase	glucose (2 mM)	[103]
Multi-layered graphene	glucose oxidase, Pt, chitosan	glucose (0.6 μM)	[104]
Multi-layered graphene	Pd nanoflower, Nafion, glucose oxidase	glucose (1 nM)	[105]
Graphene oxide	Cu nanoparticles	glucose (0.35 μM)	[107]
Reduced graphene oxide	Au-Pt alloy, chitosan-glucose oxidase	glucose (5 μM)	[108]
Graphene oxide	poly(3,4-ethylenedioxythiophene)	dopamine (0.33 μM)	[109]
Multi-layered graphene	<i>E. coli</i> O157:H7 specific antibodies	<i>E. coli</i> bacteria (10 to 100 cells/mL)	[110]
Reduced graphene oxide	Al ₂ O ₃ , Au nanoparticles	<i>E. coli</i> bacteria (100 to 100,000 cells/mL)	[111]
Reduced graphene oxide	H1N1 specific monoclonal antibodies	H1N1 influenza virus (1 to 10 ⁴ virus/mL)	[112]
Carbon paste	NiO nanoparticles, 1-butyl-3-methylimidazolium tetrafluoroborate	ascorbic acid (0.04 μM)	[27]
Graphene foam	-	NH ₃ (20 ppm), dopamine (25 nM) and selectivity measurement for chloroform, acetone, ether	[124,125,143]
Graphene foam	Co ₃ O ₄	ethanol (50 ppm; 15 ppm)	[127,130]
Graphene foam	α-Fe ₂ O ₃	NO ₂ (0.12 μM)	[131]
Graphene foam	prussian blue nanoparticles, CuNi nanoparticles, Co nanoparticles	H ₂ O ₂ (0.1 μM), glucose (2.3 μM), aminoacids (0.02mM)	[132]
Graphene foam	Au	carcinoembryonic antigen (0.024 pg/mL)	[133]
Graphene foam	Co ₃ O ₄ nanowires	glucose (25 nM)	[134]
Graphene foam	N-doped carbon nanotubes, glucose oxidase	glucose (5 μM)	[135]
Graphene foam	Ni nanoparticles	glucose (4.8 μM)	[136]
Graphene foam	Mn ₃ O ₄	glucose (10 μM), H ₂ O ₂ (1 μM)	[137]

Table 1. Cont.

Carbon Nanostructure	Functionalization	Analyte (Detection Limit)	References
Graphene foam	polydopamine, horseradish peroxidase, methylene blue	H ₂ O ₂ (58 nM)	[138]
Graphene foam	PtRu nanoparticles	H ₂ O ₂ (0.04 µM)	[139]
Graphene foam	CuO nanoparticles	glucose (1 µM)	[140]
Graphene foam	CuO nanoflower	ascorbic acid (0.43 µM)	[142]
Graphene foam	polydimethylsiloxane	human blood pressure (60 kPa ⁻¹)	[123]
Graphene foam	ZnO nanowires	uric acid (0.5 µM), dopamine (0.5 µM), ascorbic acid (5 µM)	[144]
Graphene foam	polydimethylsiloxane	strain (gauge factor 98.66)	[145,147]
Graphene foam	Polydimethylsiloxane, polyimide	strain (low pressure: 0.18 kPa ⁻¹ ; large pressure: 0.023 kPa ⁻¹)	[146]
Graphene foam-graphene quantum dots	-	Fe ³⁺ (7.22 µM)	[148]

Author Contributions: R.G.M. contributed in writing and structuring, P.S.W. contributed in writing and structuring, A.B. contributed in writing and structuring, J. S. contributed in writing and corrections, T.G. contributed to writing and corrections, Z.L. contributed in writing and corrections and M.H.R. contributed to writing and corrections.

Funding: This work is supported by the National Science Foundation China (NSFC, Project 51672181), the National Science Center for the financial support within the frame of the Sonata Program (Grant agreement 2014/13/D/ST5/02853) and the Opus program (Grant agreement 2015/19/B/ST5/03399). MHR thanks the Sino-German Research Institute for support (project: GZ 1400). SVR acknowledges NSF (ECCS-1509786).

Conflicts of Interest: The authors declare no conflict of interest.

References

- Segawa, Y.; Ito, H.; Itami, K. Structurally uniform and atomically precise carbon nanostructures. *Nat. Rev. Mater.* **2016**, *1*, 15002. [\[CrossRef\]](#)
- Vedhanarayanan, B.; Praveen, V.K.; Das, G.; Ajayaghosh, A. Hybrid materials of 1D and 2D carbon allotropes and synthetic π -systems. *NPG Asia Mater.* **2018**, *10*, 107–126. [\[CrossRef\]](#)
- Nasir, S. Carbon-Based Nanomaterials/Allotropes: A Glimpse of Their Synthesis, Properties and Some Applications. *Materials* **2018**, *11*, 259. [\[CrossRef\]](#) [\[PubMed\]](#)
- Mendes, R.G.; Bachmatiuk, A.; Büchner, B.; Cuniberti, G.; Rummeli, M.H. Carbon nanostructures as multi-functional drug delivery platforms. *J. Mater. Chem. B* **2013**, *1*, 401–428. [\[CrossRef\]](#)
- Dinadayalane, T.C.; Leszczynski, J. *Fundamental Structural, Electronic, and Chemical Properties of Carbon Nanostructures: Graphene, Fullerenes, Carbon Nanotubes, and Their Derivatives*; Leszczynski, J., Ed.; Springer: Dordrecht, The Netherlands, 2016.
- Eletsii, A.V. Mechanical properties of carbon nanostructures and related materials Mechanical properties of carbon nanostructures and related materials. *Phys. Uspekhi* **2007**, *50*, 225–265. [\[CrossRef\]](#)
- Meunier, V. Physical properties of low-dimensional sp^2 -based carbon nanostructures. *Rev. Mod. Phys.* **2016**, *88*, 1–50. [\[CrossRef\]](#)
- Lahiri, I.; Das, S.; Kang, C.; Choi, W. Application of carbon nanostructures—Energy to electronics. *J. Miner.* **2011**, *63*, 70–76. [\[CrossRef\]](#)
- Zanolli, Z.; Leghrib, R.; Felten, A.; Pireaux, J.; Llobet, E. Gas Sensing with Au-Decorated Carbon Nanotubes. *ACS Nano* **2011**, *6*, 4592–4599. [\[CrossRef\]](#)
- Rajavel, K.; Lalitha, M.; Radhakrishnan, J.K.; Senthilkumar, L.; Thangavelu, R.; Kumar, R. Multiwalled Carbon Nanotube Oxygen Sensor: Enhanced Oxygen Sensitivity at Room Temperature and Mechanism of Sensing. *ACS Appl. Mater. Interfaces* **2015**, *7*, 23857–23865. [\[CrossRef\]](#)
- Doroodmand, M.M.; Nasresfahani, S.; Sheikhi, M.H. Fabrication of ozone gas sensor based on FeOOH/single walled carbon nanotube-modified field effect transistor. *Int. J. Environ. Anal. Chem.* **2013**, *93*, 946–958. [\[CrossRef\]](#)
- Debataraja, A.; Muchtar, A.R.; Septiani, N.L.W.; Yulianto, B.; Nugraha; Sunendar, B. High Performance Carbon Monoxide Sensor Based on Nano Composite of SnO_2 -Graphene. *IEEE Sens. J.* **2017**, *17*, 8297–8305. [\[CrossRef\]](#)
- Zhang, G.; Tai, H.; Xie, G.; Jiang, Y.; Zhou, Y. A carbon monoxide sensor based on single-walled carbon nanotubes doped with copper chloride. *Sci. China Technol. Sci.* **2013**, *56*, 2576–2580. [\[CrossRef\]](#)
- Mendoza, F.; Hernández, D.M.; Makarov, V.; Febus, E.; Weiner, B.R.; Morell, G. Sensors and Actuators B: Chemical Room temperature gas sensor based on tin dioxide-carbon nanotubes composite films. *Sens. Actuators B Chem.* **2014**, *190*, 227–233. [\[CrossRef\]](#)
- Bannov, A.G.; Jašek, O.; Manakhov, A.; Márik, M.; Nečas, D.; Zajíčková, L. High-Performance Ammonia Gas Sensors Based on Plasma Treated Carbon Nanostructures. *IEEE Trans. Plasma Sci.* **2017**, *17*, 1964–1970. [\[CrossRef\]](#)
- Kumar, M.K.; Ramaprabhu, S. Nanostructured Pt Functionlized Multiwalled Carbon Nanotube Based Hydrogen Sensor. *J. Phys. Chem. B* **2006**, *110*, 11291–11298. [\[CrossRef\]](#)
- Sayago, I.; Terrado, E.; Lafuente, E.; Horrillo, M.C.; Maser, W.K.; Benito, A.M.; Navarro, R.; Urriolabeitia, E.P.; Martinez, M.T.; Gutierrez, J. Hydrogen sensors based on carbon nanotubes thin films. *Synth. Met.* **2005**, *148*, 15–19. [\[CrossRef\]](#)

18. Someya, T.; Small, J.; Kim, P.; Nuckolls, C.; Yardley, J.T. Alcohol Vapor Sensors Based on Single-Walled Carbon Nanotube Field Effect Transistors. *Nano Lett.* **2003**, *3*, 877–881. [[CrossRef](#)]
19. Chobsilp, T.; Muangrat, W.; Issro, C.; Chaiwat, W.; Eiad-ua, A.; Suttiponparnit, K.; Wongwiriyan, W.; Charinpanitkul, T. Sensitivity Enhancement of Benzene Sensor Using Ethyl Cellulose-Coated Surface-Functionalized Carbon Nanotubes. *J. Sens.* **2018**, *2018*, 6956973. [[CrossRef](#)]
20. Ngo, Y.H.; Brothers, M.; Martin, J.A.; Grigsby, C.C.; Fullerton, K.; Naik, R.R.; Kim, S.S. Chemically Enhanced Polymer-Coated Carbon Nanotube Electronic Gas Sensor for Isopropyl Alcohol Detection. *ACS Omega* **2018**, *3*, 6230–6236. [[CrossRef](#)]
21. Szkudlarek, A.; Kollbek, K.; Klejna, S.; Rydosz, A. Electronic sensitization of CuO thin films by Cr-doping for enhanced gas sensor response at low detection limit. *Mater. Res. Express* **2018**, *5*, 126406. [[CrossRef](#)]
22. Rydosz, A.; Szkudlarek, A.; Ziabka, M.; Domanski, K.; Maziarz, W.; Pisarkiewicz, T. Performance of Si-Doped WO₃ Thin Films for Acetone Sensing Prepared by Glancing Angle DC Magnetron Sputtering. *IEEE Sens. J.* **2016**, *16*, 1004–1012. [[CrossRef](#)]
23. Zhang, J.; Zhu, Q.; Zhang, Y.; Zhu, Z.; Liu, Q. Methanol Gas-Sensing Properties of SWCNT-MIP Composites. *Nanoscale Res. Lett.* **2016**, *11*, 522. [[CrossRef](#)] [[PubMed](#)]
24. Cash, K.J.; Clark, H.A. Nanosensors and nanomaterials for monitoring glucose in diabetes. *Trends Mol. Med.* **2010**, *16*, 584–593. [[CrossRef](#)] [[PubMed](#)]
25. Rahim, A.; Rehman, Z.U.; Mir, S.; Muhammad, N.; Rehman, F.; Nawaz, M.H.; Yaqub, M.; Siddiqi, S.A.; Chaudhry, A.A. A non-enzymatic glucose sensor based on CuO-nanostructure modified carbon ceramic electrode. *J. Mol. Liq.* **2017**, *248*, 425–431. [[CrossRef](#)]
26. Sainio, S.; Palomäki, T.; Tujunen, N.; Protopopova, V.; Koehne, J.; Kordas, K.; Koskinen, J.; Meyyappan, M.; Laurila, T. Integrated Carbon Nanostructures for Detection of Neurotransmitters. *Mol. Neurobiol.* **2015**, *52*, 859–866. [[CrossRef](#)]
27. Pardakhty, A.; Ahmadzadeh, S.; Avazpour, S.; Kumar, V. Highly sensitive and efficient voltammetric determination of ascorbic acid in food and pharmaceutical samples from aqueous solutions based on nanostructure carbon paste electrode as a sensor. *J. Mol. Liq.* **2016**, *216*, 387–391. [[CrossRef](#)]
28. Tahira, A.; Nafady, A.; Baloach, Q.; Sirajuddin; Sherazi, S.T.H.; Shaikh, T.; Arain, M.; Willander, M.; Hussain, Z. Ascorbic Acid Assisted Synthesis of Cobalt Oxide Nanostructures, Their Electrochemical Sensing Application for the Sensitive Determination of Hydrazine. *J. Electron. Mater.* **2016**, *45*, 3695–3701. [[CrossRef](#)]
29. Wu, W.; Min, H.; Wu, H.; Ding, Y.; Yang, S. Electrochemical Determination of Uric Acid Using a Multiwalled Carbon Nanotube Platinum–Nickel Alloy Glassy Carbon Electrode. *Electrochemistry* **2017**, *50*, 91–104. [[CrossRef](#)]
30. Chen, H.; Zhang, Z.; Cai, D.; Zhang, S.; Zhang, B.; Tang, J.; Wu, Z. Talanta A hydrogen peroxide sensor based on Ag nanoparticles electrodeposited on natural nano-structure attapulgite modified glassy carbon electrode. *Talanta* **2011**, *86*, 266–270. [[CrossRef](#)] [[PubMed](#)]
31. Hu, P.; Zhang, J.; Li, L.; Wang, Z.; Estrela, P. Carbon Nanostructure-Based Field-Effect Transistors for Label-Free Chemical/Biological Sensors. *Sensors* **2010**, *10*, 5133–5159. [[CrossRef](#)]
32. Stetter, J.R.; Penrose, W.R.; Yao, S. Sensors, Chemical Sensors, Electrochemical Sensors, and ECS. *J. Electrochem. Soc.* **2003**, *150*, S11–S16. [[CrossRef](#)]
33. Jiménez-Cadena, G.; Riu, J.; Rius, F.X. Gas sensors based on nanostructured materials. *Analyst* **2007**, *132*, 1083–1099. [[CrossRef](#)] [[PubMed](#)]
34. Septiani, N.L.W.; Yulianto, B. Review—The Development of Gas Sensor Based on Carbon Nanotubes. *J. Electrochem. Soc.* **2016**, *163*, B97–B106. [[CrossRef](#)]
35. Chavan, R.; Desai, U.; Mhatre, P.; Chinchole, R. A review: Carbon nanotubes. *Int. J. Pharm. Sci. Rev. Res.* **2012**, *13*, 124–134. [[CrossRef](#)]
36. Baptista, F.R.; Belhout, S.A.; Giordani, S.; Quinn, S.J. Recent developments in carbon nanomaterial sensors. *Chem. Soc. Rev.* **2015**, *44*, 4433–4453. [[CrossRef](#)]
37. Llobet, E. Gas sensors using carbon nanomaterials: A review. *Sens. Actuators B Chem.* **2013**, *179*, 32–45. [[CrossRef](#)]
38. Liu, H.; Zhang, L.; Yan, M.; Yu, J. Carbon nanostructures in biology and medicine. *J. Mater. Chem. B* **2017**, *5*, 6437–6450. [[CrossRef](#)]
39. Idowu, A.; Boesl, B.; Agarwal, A. 3D graphene foam-reinforced polymer composites—A review. *Carbon N. Y.* **2018**, *135*, 52–71. [[CrossRef](#)]

40. Sha, J.; Gao, C.; Lee, S.K.; Li, Y.; Zhao, N.; Tour, J.M. Preparation of three-dimensional graphene foams using powder metallurgy templates. *ACS Nano* **2016**, *10*, 1411–1416. [[CrossRef](#)] [[PubMed](#)]
41. Yao, X.; Zhao, Y. Three-Dimensional Porous Graphene Networks and Hybrids for Lithium-Ion Batteries and Supercapacitors. *Chem* **2017**, *2*, 171–200. [[CrossRef](#)]
42. Olszowska, K.; Pang, J.; Wrobel, P.S.; Zhao, L.; Ta, H.Q.; Liu, Z.; Trzebicka, B.; Bachmatiuk, A.; Rummeli, M.H. Three-dimensional nanostructured graphene: Synthesis and energy, environmental and biomedical applications. *Synth. Met.* **2017**, *234*, 53–85. [[CrossRef](#)]
43. Iijima, S. Helical microtubules of graphitic carbon. *Nature* **1991**, *354*, 56–58. [[CrossRef](#)]
44. Dresselhaus, M.S.; Dresselhaus, G.; Avouris, P. *Carbon Nanotubes: Synthesis, Properties, and Applications*; Springer: Berlin, Germany, 2001; ISBN 3540410864.
45. De Volder, M.F.L.; Tawfick, S.H.; Baughman, R.H.; Hart, A.J. Carbon Nanotubes: Present and Future Commercial Applications. *Science* **2013**, *339*, 535–540. [[CrossRef](#)] [[PubMed](#)]
46. Ajayan, P.M. Nanotubes from Carbon. *Chem. Rev.* **1999**, *7*, 1787–1800. [[CrossRef](#)]
47. Peigney, A.; Laurent, C.; Flahaut, E.; Bacsa, R.R.; Rousset, A. Specific surface area of carbon nanotubes and bundles of carbon nanotubes. *Carbon* **2001**, *39*, 507–514. [[CrossRef](#)]
48. Collins, P.G.; Bradley, K.; Ishigami, M.; Zettl, A. Extreme Oxygen Sensitivity of Electronic Properties of Carbon Nanotubes. *Science* **2000**, *287*, 1801–1805. [[CrossRef](#)] [[PubMed](#)]
49. Wang, Y.; Zhou, Z.; Yang, Z.; Chen, X.; Xu, D. Gas sensors based on deposited single-walled carbon nanotube networks for DMMP detection. *Nanotechnology* **2009**. [[CrossRef](#)] [[PubMed](#)]
50. Valentini, L.; Armentano, I.; Kenny, J.M.; Cantalini, C.; Lozzi, L.; Santucci, S. Sensors for sub-ppm NO₂ gas detection based on carbon nanotube thin films. *Appl. Phys. Lett.* **2003**, *82*, 961–963. [[CrossRef](#)]
51. Ueda, T.; Bhuiyan, M.M.H.; Norimatsu, H.; Katsuki, S.; Ikegami, T.; Mitsugi, F. Development of carbon nanotube-based gas sensors for NO_x gas detection working at low temperature. *Phys. E Low Dimens. Syst. Nanostruct.* **2008**, *40*, 2272–2277. [[CrossRef](#)]
52. Higginbotham, A.L.; Kosynkin, D.V.; Sinitskii, A.; Sun, Z.; Tour, J.M. Lower-Defect Graphene Oxide Nanoribbons from Multiwalled Carbon Nanotubes. *ACS Nano* **2010**, *4*, 2059–2069. [[CrossRef](#)] [[PubMed](#)]
53. Dutko, O.; Plachá, D.; Mikeska, M.; Martynková, G.S.; Wróbel, P.; Bachmatiuk, A.; Rummeli, M.H. Comparison of Selected Oxidative Methods for Carbon Nanotubes: Structure and Functionalization Study. *J. Nanosci. Nanotechnol.* **2016**, *16*, 7822–7825. [[CrossRef](#)]
54. Scheibe, B.; Borowiak-Palen, E.; Kalenczuk, R.J. Oxidation and reduction of multiwalled carbon nanotubes—Preparation and characterization. *Mater. Charact.* **2010**, *61*, 185–191. [[CrossRef](#)]
55. Čech, J.; Curran, S.A.; Zhang, D.; Dewald, J.L.; Avadhanula, A.; Kandadai, M.; Roth, S. Functionalization of multi-walled carbon nanotubes: Direct proof of sidewall thiolation. *Phys. Status Solidi B* **2006**, *322S*, 3221–3225. [[CrossRef](#)]
56. Lim, J.K.; Yun, W.S.; Yoon, M.; Lee, S.K.; Kim, C.H.; Kim, K.; Kim, S.K. Selective thiolation of single-walled carbon nanotubes. *Synth. Met.* **2003**, *139*, 521–527. [[CrossRef](#)]
57. Curran, S.A.; Cech, J.; Zhang, D.; Dewald, J.L.; Avadhanula, A.; Kandadai, M.; Roth, S. Thiolation of carbon nanotubes and sidewall functionalization. *J. Mater. Res.* **2006**, *21*, 1012–1018. [[CrossRef](#)]
58. Hines, D.; Rummeli, M.H.; Adebimpe, D.; Akins, D.L. High-yield photolytic generation of brominated single-walled carbon nanotubes and their application for gas sensing. *Chem. Commun.* **2014**, *50*, 11568–11571. [[CrossRef](#)] [[PubMed](#)]
59. Sayogo, I.; Santos, H.; Horrilo, M.; Aleixandre, M.; Fernandez, M.; Terrado, E.; Tacchini, I.; Aroz, R.; Maser, W.; Benito, A.; et al. Carbon nanotube networks as gas sensors for NO₂ detection. *Talanta* **2008**, *77*, 758–764. [[CrossRef](#)]
60. Guo, M.A.; Xu, M.E.; Pan, M.; Chen, Y.Q. Effect of thiol on formaldehyde sensors based on CNTs. In Proceedings of the 2009 3rd International Conference on Bioinformatics and Biomedical Engineering, Beijing, China, 11–13 June 2009; Volume 1–11, pp. 3793–3795.
61. Xie, H.; Sheng, C.; Chen, X.; Wang, X.; Li, Z.; Zhou, J. Multi-wall carbon nanotube gas sensors modified with amino-group to detect low concentration of formaldehyde. *Sens. Actuators B Chem.* **2012**, *168*, 34–38. [[CrossRef](#)]
62. Zhang, T.; Mubeen, S.; Myung, N.V.; Deshusses, M.A. Recent progress in carbon nanotube-based gas sensors. *Nanotechnology* **2008**, *19*, 332001. [[CrossRef](#)]

63. Kong, J.; Franklin, N.R.; Zhou, C.; Chapline, M.G.; Peng, S.; Cho, K.; Dai, H.; Chongwu, Z.; Chapline, M.G.; Peng, S.; et al. Nanotube Molecular Wires as Chemical Sensors. *Science* **2000**, *287*, 622–625. [[CrossRef](#)]
64. Shimizu, Y.; Egashira, M. Basic aspects and challenges of semiconductor gas sensors. *J. MRS Bull.* **1999**, *24*, 18–24. [[CrossRef](#)]
65. Star, A.; Joshi, V.; Skarupo, S.; Thomas, D.; Gabriel, J.P.; Emery, V. Gas Sensor Array Based on Metal-Decorated Carbon Nanotubes. *J. Phys. Chem. B* **2006**, *110*, 21014–21020. [[CrossRef](#)] [[PubMed](#)]
66. Novak, J.P.; Snow, E.S.; Houser, E.J.; Park, D.; Stepnowski, J.L.; McGill, R.A. Nerve agent detection using networks of single-walled carbon nanotubes. *Appl. Phys. Lett.* **2003**, *83*, 4026–4028. [[CrossRef](#)]
67. Lin, Y.; Lu, F.; Tu, Y.; Ren, Z. Glucose Biosensors Based on Carbon Nanotube Nanoelectrode Ensembles. *Nano Lett.* **2004**, *4*, 191–195. [[CrossRef](#)]
68. Liu, X.; Shi, L.; Niu, W.; Li, H.; Xu, G. Amperometric glucose biosensor based on single-walled carbon nanohorns. *Biosens. Bioelectron.* **2008**, *23*, 1887–1890. [[CrossRef](#)] [[PubMed](#)]
69. Yao, Y.L.; Shiu, K.K. A mediator-free bienzyme amperometric biosensor based on horseradish peroxidase and glucose oxidase immobilized on carbon nanotube modified electrode. *Electroanalysis* **2008**, *20*, 2090–2095. [[CrossRef](#)]
70. Zhao, K.; Zhuang, S.; Chang, Z.; Songm, H.; Dai, L.; He, P.; Fang, Y. Amperometric Glucose Biosensor Based on Platinum Nanoparticles Combined Aligned Carbon Nanotubes Electrode. *Electroanalysis* **2007**, *19*, 1069–1074. [[CrossRef](#)]
71. Wang, J.; Tangkuaram, T.; Loyprasert, S.; Vazquez-Alvarez, T.; Veerasai, W.; Kanatharana, P.; Thavarungkul, P. Electrocatalytic detection of insulin at RuOx/carbon nanotube-modified carbon electrodes. *Anal. Chim. Acta* **2007**, *581*, 1–6. [[CrossRef](#)]
72. Martínez-Periñán, E.; Revenga-Parra, M.; Gennari, M.; Pariente, F.; Mas-Ballesté, R.; Zamora, F.; Lorenzo, E. Insulin sensor based on nanoparticle-decorated multiwalled carbon nanotubes modified electrodes. *Sens. Actuators B Chem.* **2016**, *222*, 331–338. [[CrossRef](#)]
73. Swamy, B.E.K.; Venton, B.J. Carbon nanotube-modified microelectrodes for simultaneous detection of dopamine and serotonin in vivo. *Analyst* **2007**, *132*, 876–884. [[CrossRef](#)]
74. Sun, Y.; Fei, J.; Hou, J.; Zhang, Q. Simultaneous determination of dopamine and serotonin using a carbon nanotubes-ionic liquid gel modified glassy carbon electrode. *Microchim. Acta* **2009**, *165*, 373–379. [[CrossRef](#)]
75. Novoselov, K.S.; Geim, A.K.; Morozov, S.V.; Jiang, D.; Zhang, Y.; Dubonos, S.V.; Grigorieva, I.V.; Firsov, A.A. Electric Field Effect in Atomically Thin Carbon Films. *Science* **2004**, *306*, 666–669. [[CrossRef](#)] [[PubMed](#)]
76. Geim, A.K.; Novoselov, K.S. The rise of graphene. *Nat. Mater.* **2007**, *6*, 183–191. [[CrossRef](#)]
77. Bonaccorso, F.; Colombo, L.; Yu, G.; Stoller, M.; Tozzini, V.; Ferrari, A.C.; Ruoff, R.S.; Pellegrini, V. Graphene, related two-dimensional crystals, and hybrid systems for energy conversion and storage. *Science* **2015**, *347*. [[CrossRef](#)] [[PubMed](#)]
78. Dreyer, D.R.; Park, S.; Bielawski, W.; Ruoff, R.S. The chemistry of graphene oxide. *Chem. Soc. Rev.* **2010**, *39*, 228–240. [[CrossRef](#)] [[PubMed](#)]
79. Yang, D.; Velamakanni, A.; Bozoklu, G.; Park, S.; Stoller, M.; Piner, R.D.; Stankovich, S.; Jung, I.; Field, D.A.; Ventrice, C.A., Jr.; et al. Chemical analysis of graphene oxide films after heat and chemical treatments by X-ray photoelectron and Micro-Raman spectroscopy. *Carbon N. Y.* **2009**, *47*, 145–152. [[CrossRef](#)]
80. Li, X.; Zhu, Y.; Cai, W.; Borysiak, M.; Han, B.; Chen, D.; Piner, R.D.; Colombo, L.; Ruoff, R.S. Transfer of Large-Area Graphene Films for High-Performance Transparent Conductive Electrodes. *Nano Lett.* **2009**, *9*, 4359–4363. [[CrossRef](#)]
81. Becerril, H.A.; Mao, J.; Liu, Z.; Stoltenberg, R.M.; Bao, Z.; Chen, Y. Evaluation of Solution-Processed Reduced Graphene Oxide Films as Transparent Conductors. *ACS Nano* **2008**, *2*, 463–470. [[CrossRef](#)]
82. Ko, G.; Kim, H.-Y.; Ahn, J.; Park, Y.-M.; Lee, K.-Y.; Kim, J. Graphene-based nitrogen dioxide gas sensors. *Curr. Appl. Phys.* **2010**, *10*, 1002–1004. [[CrossRef](#)]
83. Pearce, R.; Iakimov, T.; Andersson, M.; Hultman, L.; Spetz, A.L.; Yakimova, R. Epitaxially grown graphene based gas sensors for ultra sensitive NO₂ detection. *Sens. Actuators B Chem.* **2011**, *155*, 451–455. [[CrossRef](#)]
84. Yavari, F.; Castillo, E.; Gullapalli, H.; Ajayan, P.M.; Koratkar, N. High sensitivity detection of NO₂ and NH₃ in air using chemical vapor deposition grown graphene. *Appl. Phys. Lett.* **2012**, *100*, 203120. [[CrossRef](#)]
85. Miasik, J.J.; Hooper, A.; Tofield, B.C. Conducting polymer gas sensors. *J. Chem. Soc. Faraday Trans. 1 Phys. Chem. Condens. Phases* **1986**, *82*, 1117–1126. [[CrossRef](#)]

86. Choi, H.; Jeong, H.Y.; Lee, D.; Choi, C.-G.; Choi, S. Flexible NO₂ gas sensor using multilayer graphene films by chemical vapor deposition. *Carbon Lett.* **2013**, *14*, 186–189. [[CrossRef](#)]
87. Yoon, H.J.; Jun, D.H.; Yang, J.H.; Zhou, Z.; Yang, S.S.; Cheng, M.M.-C. Carbon dioxide gas sensor using a graphene sheet. *Sens. Actuators B Chem.* **2011**, *157*, 310–313. [[CrossRef](#)]
88. Nemade, K.R.; Waghuley, S.A. Chemiresistive Gas Sensing by Few-Layered Graphene. *J. Electron. Mater.* **2013**, *42*, 2857–2866. [[CrossRef](#)]
89. Schedin, F.; Geim, A.K.; Morozov, S.V.; Hill, E.W.; Blake, P.; Katsnelson, M.I.; Novoselov, K.S. Detection of individual gas molecules adsorbed on graphene. *Nat. Mater.* **2007**, *6*, 652–655. [[CrossRef](#)] [[PubMed](#)]
90. Gautam, M.; Jayatissa, A.H. Graphene based field effect transistor for the detection of ammonia. *J. Appl. Phys.* **2012**, *112*, 064304. [[CrossRef](#)]
91. Prezioso, S.; Perrozzi, F.; Giancaterini, L.; Cantalini, C.; Treossi, E.; Palermo, V.; Nardone, M.; Santucci, S.; Ottaviano, L. Graphene Oxide as a Practical Solution to High Sensitivity Gas Sensing. *J. Phys. Chem.* **2013**, *117*, 10683–10690. [[CrossRef](#)]
92. Taylor, A.P.; Velásquez-garcía, L.F. Electrospray-printed nanostructured graphene oxide gas sensors. *Nanotechnology* **2015**, *26*, 505301. [[CrossRef](#)]
93. Wróbel, P.; Włodarski, M.; Jedrzejewska, A.; Placek, K.; Szukiewicz, R.; Kotowicz, S.; Tokarska, K.; Ta, H.Q.; Mendes, R.G.; Liu, Z.; et al. A comparative study on simple and practical chemical gas sensors from chemically modified graphene films. *Mater. Res. Express* **2018**, *6*, 1. [[CrossRef](#)]
94. Fowler, J.D.; Allen, K.M.J.; Tung, K.V.C.; Yang, Y.; Kaner, R.B.; Weiller, B.H. Practical Chemical Sensors from Chemically Derived Graphene. *ACS Nano* **2009**, *3*, 301–306. [[CrossRef](#)] [[PubMed](#)]
95. Lu, G.; Ocola, L.E.; Chen, J. Gas detection using low-temperature reduced graphene oxide sheets. *Appl. Phys. Lett.* **2009**, *94*, 083111. [[CrossRef](#)]
96. Lu, G.; Park, S.; Yu, K.; Ruoff, R.S.; Ocola, L.E.; Rosenmann, D.; Chen, J. Toward practical gas sensing with highly reduced graphene oxide: A new signal processing method to circumvent run-to-run and device-to-device variations. *ACS Nano* **2011**, *5*, 1154–1164. [[CrossRef](#)] [[PubMed](#)]
97. Lu, G.; Ocola, L.E.; Chen, J. Reduced graphene oxide for room-temperature gas sensors. *Nanotechnology* **2009**, *20*, 44. [[CrossRef](#)] [[PubMed](#)]
98. Dua, V.; Surwade, S.P.; Ammu, S.; Agnihotra, S.R.; Jain, S.; Roberts, K.E.; Park, S.; Ruoff, R.S.; Manohar, S.K. All-Organic Vapor Sensor Using Inkjet-Printed Reduced Graphene Oxide. *Angew. Chem. Int. Ed.* **2010**, *49*, 2154–2157. [[CrossRef](#)] [[PubMed](#)]
99. Park, H.J.; Kim, W.-J.; Lee, H.-K.; Lee, D.-S.; Shin, J.-H.; Jun, Y.; Yun, Y.J. Highly flexible, mechanically stable, and sensitive NO₂ gas sensors based on reduced graphene oxide nanofibrous mesh fabric for flexible electronics. *Sens. Actuators B Chem.* **2018**, *257*, 846–852. [[CrossRef](#)]
100. Lipatov, A.; Varezchnikov, A.; Wilson, P.; Sysoev, V.; Kolmakov, A.; Sinitskii, A. Highly selective gas sensor arrays based on thermally reduced graphene oxide. *Nanoscale* **2013**, *5*, 5426–5434. [[CrossRef](#)] [[PubMed](#)]
101. Yuan, W.; Liu, A.; Huang, L.; Li, C.; Shi, G. High-Performance NO₂ Sensors Based on Chemically Modified Graphene. *Adv. Mater.* **2013**, *25*, 766–771. [[CrossRef](#)]
102. Zöpfl, A.; Lemberger, M.; König, M.; Ruhl, G.; Matysik, F.; Hirsch, T. Reduced graphene oxide and graphene composite materials for improved gas sensing at low temperature. *Faraday Discuss.* **2014**, *173*, 403–414. [[CrossRef](#)]
103. Shan, C.; Yang, H.; Song, J.; Han, D.; Ivaska, A.; Niu, L. Direct Electrochemistry of Glucose Oxidase and Biosensing for Glucose Based on Graphene. *Anal. Chem.* **2009**, *81*, 2378–2382. [[CrossRef](#)]
104. Wu, H.; Wang, J.; Kang, X.; Wang, C.; Wang, D.; Liu, J.; Aksay, I.A.; Lin, Y. Talanta Glucose biosensor based on immobilization of glucose oxidase in platinum nanoparticles/graphene/chitosan nanocomposite film. *Talanta* **2009**, *80*, 403–406. [[CrossRef](#)] [[PubMed](#)]
105. Shin, D.H.; Kima, W.; Jun, J.; Lee, J.S.; Kim, J.H.; Jang, J. Highly selective FET-type glucose sensor based on shape-controlled palladium nanoflower-decorated graphene. *Sens. Actuators B Chem.* **2018**, *264*, 216–223. [[CrossRef](#)]
106. Meng, L.; Jin, J.; Yang, G.; Lu, T.; Zhang, H.; Cai, C. Nonenzymatic Electrochemical Detection of Glucose Based on Palladium–Single-Walled Carbon Nanotube Hybrid Nanostructures. *Anal. Chem.* **2009**, *81*, 7271–7280. [[CrossRef](#)] [[PubMed](#)]

107. Lin, S.; Feng, W.; Miao, X.; Zhang, X.; Chen, S.; Chen, Y.; Wang, W.; Zhang, Y. A flexible and highly sensitive nonenzymatic glucose sensor based on DVD-laser scribed graphene substrate. *Biosens. Bioelectron.* **2018**, *110*, 89–96. [[CrossRef](#)] [[PubMed](#)]
108. Xuan, X.; Yoon, H.S.; Park, J.Y. A wearable electrochemical glucose sensor based on simple and low-cost fabrication supported micro-patterned reduced graphene oxide nanocomposite electrode on flexible substrate. *Biosens. Bioelectron.* **2018**, *109*, 75–82. [[CrossRef](#)] [[PubMed](#)]
109. Xu, G.; Jarjes, Z.A.; Desprez, V.; Kilmartin, P.A.; Travas-Sejdic, J. Sensitive, selective, disposable electrochemical dopamine sensor based on PEDOT-modified laser scribed graphene. *Biosens. Bioelectron.* **2018**, *107*, 184–191. [[CrossRef](#)]
110. Pandey, A.; Gurbuz, Y.; Ozguz, V.; Niazi, J.H.; Qureshi, A. Graphene-interfaced electrical biosensor for label-free and sensitive detection of foodborne pathogenic E. coli O157:H7. *Biosens. Bioelectron.* **2017**, *91*, 225–231. [[CrossRef](#)]
111. Thakur, B.; Zhou, G.; Chang, J.; Pu, H.; Jin, B.; Sui, X.; Yuan, X.; Yang, C.-H.; Magruder, M.; Chen, J. Rapid detection of single E. coli bacteria using a graphene-based field-effect transistor device. *Biosens. Bioelectron.* **2018**, *110*, 16–22. [[CrossRef](#)]
112. Singh, R.; Hong, S.; Jang, J. Label-free Detection of Influenza Viruses using a Reduced Graphene Oxide-based Electrochemical Immunosensor Integrated with a Microfluidic Platform. *Sci. Rep.* **2017**, *7*, 1–11. [[CrossRef](#)]
113. Geim, A.K. Graphene: Status and Prospects. *Science* **2014**, *1530*, 1530–1534. [[CrossRef](#)]
114. Georgios, D.K.; Emmanuel, T.; George, F.E.; Maroulis, G.; Simos, T.E. Pillared Graphene: A New 3-D Innovative Network Nanostructure Augments Hydrogen Storage. *AIP Conf. Proc.* **2009**, *1148*, 388–391. [[CrossRef](#)]
115. Chen, Z.; Ren, W.; Gao, L.; Liu, B.; Pei, S.; Cheng, H.M. Three-dimensional flexible and conductive interconnected graphene networks grown by chemical vapour deposition. *Nat. Mater.* **2011**, *10*, 424–428. [[CrossRef](#)] [[PubMed](#)]
116. Worsley, M.A.; Kucheyev, S.O.; Mason, H.E.; Merrill, M.D.; Mayer, B.P.; Lewicki, J.; Valdez, C.A.; Suss, M.E.; Stadermann, M.; Pauzauskie, P.J.; et al. Mechanically robust 3D graphene macroassembly with high surface area. *Chem. Commun.* **2012**, *48*, 8428–8430. [[CrossRef](#)] [[PubMed](#)]
117. Xia, Z.Y.; Wei, D.; Anitowska, E.; Bellani, V.; Ortolani, L.; Morandi, V.; Gazzano, M.; Zanelli, A.; Borini, S.; Palermo, V. Electrochemically exfoliated graphene oxide/iron oxide composite foams for lithium storage, produced by simultaneous graphene reduction and Fe(OH)₃ condensation. *Carbon N. Y.* **2015**, *84*, 254–262. [[CrossRef](#)]
118. Qiu, L.; Liu, J.Z.; Chang, S.L.Y.; Wu, Y.; Li, D. Biomimetic superelastic graphene-based cellular monoliths. *Nat. Commun.* **2012**, *3*, 1241. [[CrossRef](#)] [[PubMed](#)]
119. Hydrogel, S.G. Self-Assembled Graphene Hydrogel. *ACS Nano* **2010**, *4*, 4324–4330. [[CrossRef](#)]
120. Worsley, M.A.; Pham, T.T.; Yan, A.; Shin, S.J.; Lee, J.R.I.; Bagge-Hansen, M.; Mickelson, W.; Zettl, A. Synthesis and characterization of highly crystalline graphene aerogels. *ACS Nano* **2014**, *8*, 11013–11022. [[CrossRef](#)]
121. Wu, C.; Fang, L.; Huang, X.; Jiang, P. Three-dimensional highly conductive graphene-silver nanowire hybrid foams for flexible and stretchable conductors. *ACS Appl. Mater. Interfaces* **2014**, *6*, 21026–21034. [[CrossRef](#)]
122. Yao, H.B.; Ge, J.; Wang, C.F.; Wang, X.; Hu, W.; Zheng, Z.J.; Ni, Y.; Yu, S.H. A flexible and highly pressure-sensitive graphene-polyurethane sponge based on fractured microstructure design. *Adv. Mater.* **2013**, *25*, 6692–6698. [[CrossRef](#)]
123. Samad, Y.A.; Li, Y.; Alhassan, S.M.; Liao, K. Novel graphene foam composite with adjustable sensitivity for sensor applications. *ACS Appl. Mater. Interfaces* **2015**, *7*, 9196–9202. [[CrossRef](#)]
124. Yavari, F.; Chen, Z.; Thomas, A.V.; Ren, W.; Cheng, H.M.; Koratkar, N. High sensitivity gas detection using a macroscopic three-dimensional graphene foam network. *Sci. Rep.* **2011**, *1*, 1–5. [[CrossRef](#)] [[PubMed](#)]
125. Hua, H.; Xie, X.; Sun, J.; Qin, G.; Tang, C.; Zhang, Z.; Ding, Z.; Yue, W. Graphene foam chemical sensor system based on principal component analysis and backpropagation neural network. *Adv. Condens. Matter Phys.* **2018**, *2018*, 2361571. [[CrossRef](#)]
126. Mei, W.; Huang, J.; Zhu, L.; Ye, Z.; Mai, Y.; Tu, J. Synthesis of porous rhombus-shaped Co₃O₄ nanorod arrays grown directly on a nickel substrate with high electrochemical performance. *J. Mater. Chem.* **2012**, *22*, 9315–9321. [[CrossRef](#)]

127. Cao, A.M.; Hu, J.S.; Liang, H.P.; Song, W.G.; Wan, L.J.; He, X.L.; Gao, X.G.; Xia, S.H. Hierarchically structured cobalt oxide (Co_3O_4): The morphology control and its potential in sensors. *J. Phys. Chem. B* **2006**, *110*, 15858–15863. [[CrossRef](#)] [[PubMed](#)]
128. Vladimirova, S.; Krivetskiy, V.; Rumyantseva, M.; Gaskov, A.; Mordvinova, N.; Lebedev, O.; Martyshev, M.; Forsh, P. Co_3O_4 as p-type material for CO sensing in humid air. *Sensors* **2017**, *17*, 2216. [[CrossRef](#)]
129. Patil, D.; Patil, P.; Subramanian, V.; Joy, P.A.; Potdar, H.S. Highly sensitive and fast responding CO sensor based on Co_3O_4 nanorods. *Talanta* **2010**, *81*, 37–43. [[CrossRef](#)] [[PubMed](#)]
130. Li, L.; Liu, M.; He, S.; Chen, W. Freestanding 3D mesoporous Co_3O_4 @carbon foam nanostructures for ethanol gas sensing. *Anal. Chem.* **2014**, *86*, 7996–8002. [[CrossRef](#)] [[PubMed](#)]
131. Ma, Y.; Song, X.; Ge, X.; Zhang, H.; Wang, G.; Zhang, Y.; Zhao, H. In situ growth of $\alpha\text{-Fe}_2\text{O}_3$ nanorod arrays on 3D carbon foam as an efficient binder-free electrode for highly sensitive and specific determination of nitrite. *J. Mater. Chem. A* **2017**, *5*, 4726–4736. [[CrossRef](#)]
132. Wang, L.; Zhang, Q.; Chen, S.; Xu, F.; Chen, S.; Jia, J.; Tan, H.; Hou, H.; Song, Y. Electrochemical sensing and biosensing platform based on biomass-derived macroporous carbon materials. *Anal. Chem.* **2014**, *86*, 1414–1421. [[CrossRef](#)]
133. Lin, D.; Wu, J.; Ju, H.; Yan, F. Nanogold/mesoporous carbon foam-mediated silver enhancement for graphene-enhanced electrochemical immunosensing of carcinoembryonic antigen. *Biosens. Bioelectron.* **2014**, *52*, 153–158. [[CrossRef](#)]
134. Dong, X.C.; Xu, H.; Wang, X.W.; Huang, Y.X.; Chan-Park, M.B.; Zhang, H.; Wang, L.H.; Huang, W.; Chen, P. 3D graphene-cobalt oxide electrode for high-performance supercapacitor and enzymeless glucose detection. *ACS Nano* **2012**, *6*, 3206–3213. [[CrossRef](#)] [[PubMed](#)]
135. Fan, P.; Liu, L.; Guo, Q.; Wang, J.; Yang, J.; Guan, X.; Chen, S.; Hou, H. Three-dimensional N-doped carbon nanotube@carbon foam hybrid: An effective carrier of enzymes for glucose biosensors. *RSC Adv.* **2017**, *7*, 26574–26582. [[CrossRef](#)]
136. Wang, L.; Zhang, Y.; Yu, J.; He, J.; Yang, H.; Ye, Y.; Song, Y. A green and simple strategy to prepare graphene foam-like three-dimensional porous carbon/Ni nanoparticles for glucose sensing. *Sens. Actuators B Chem.* **2017**, *239*, 172–179. [[CrossRef](#)]
137. Si, P.; Dong, X.C.; Chen, P.; Kim, D.H. A hierarchically structured composite of Mn_3O_4 /3D graphene foam for flexible nonenzymatic biosensors. *J. Mater. Chem. B* **2013**, *1*, 110–115. [[CrossRef](#)]
138. Liu, J.; Wang, T.; Wang, J.; Wang, E. Mussel-inspired biopolymer modified 3D graphene foam for enzyme immobilization and high performance biosensor. *Electrochim. Acta* **2015**, *161*, 17–22. [[CrossRef](#)]
139. Kung, C.C.; Lin, P.Y.; Buse, F.J.; Xue, Y.; Yu, X.; Dai, L.; Liu, C.C. Preparation and characterization of three dimensional graphene foam supported platinum-ruthenium bimetallic nanocatalysts for hydrogen peroxide based electrochemical biosensors. *Biosens. Bioelectron.* **2014**, *52*, 1–7. [[CrossRef](#)]
140. Hsu, Y.W.; Hsu, T.K.; Sun, C.L.; Nien, Y.T.; Pu, N.W.; Ger, M. Der Synthesis of CuO /graphene nanocomposites for nonenzymatic electrochemical glucose biosensor applications. *Electrochim. Acta* **2012**, *82*, 152–157. [[CrossRef](#)]
141. Jindal, K.; Tomar, M.; Gupta, V. CuO thin film based uric acid biosensor with enhanced response characteristics. *Biosens. Bioelectron.* **2012**, *38*, 11–18. [[CrossRef](#)]
142. Ma, Y.; Zhao, M.; Cai, B.; Wang, W.; Ye, Z.; Huang, J. 3D graphene foams decorated by CuO nanoflowers for ultrasensitive ascorbic acid detection. *Biosens. Bioelectron.* **2014**, *59*, 384–388. [[CrossRef](#)]
143. Dong, X.; Wang, X.; Wang, L.; Song, H.; Zhang, H.; Huang, W.; Chen, P. 3D graphene foam as a monolithic and macroporous carbon electrode for electrochemical sensing. *ACS Appl. Mater. Interfaces* **2012**, *4*, 3129–3133. [[CrossRef](#)]
144. Yue, H.Y.; Huang, S.; Chang, J.; Heo, C.; Yao, F.; Adhikari, S.; Gunes, F.; Liu, L.C.; Lee, T.H.; Oh, E.S.; et al. ZnO nanowire arrays on 3D hierarchical graphene foam: Biomarker detection of parkinson's disease. *ACS Nano* **2014**, *8*, 1639–1646. [[CrossRef](#)] [[PubMed](#)]
145. Xu, R.; Lu, Y.; Jiang, C.; Chen, J.; Mao, P.; Gao, G.; Zhang, L.; Wu, S. Facile fabrication of three-dimensional graphene foam/poly(dimethylsiloxane) composites and their potential application as strain sensor. *ACS Appl. Mater. Interfaces* **2014**, *6*, 13455–13460. [[CrossRef](#)] [[PubMed](#)]
146. Qin, Y.; Peng, Q.; Ding, Y.; Lin, Z.; Wang, C.; Li, Y.; Xu, F.; Li, J.; Yuan, Y.; He, X.; et al. Lightweight, Superelastic, and Mechanically Flexible Graphene/Polyimide Nanocomposite Foam for Strain Sensor Application. *ACS Nano* **2015**, *9*, 8933–8941. [[CrossRef](#)] [[PubMed](#)]

147. Li, J.; Zhao, S.; Zeng, X.; Huang, W.; Gong, Z.; Zhang, G.; Sun, R.; Wong, C.P. Highly Stretchable and Sensitive Strain Sensor Based on Facilely Prepared Three-Dimensional Graphene Foam Composite. *ACS Appl. Mater. Interfaces* **2016**, *8*, 18954–18961. [[CrossRef](#)] [[PubMed](#)]
148. Ananthanarayanan, A.; Wang, X.; Routh, P.; Sana, B.; Lim, S.; Kim, D.H.; Lim, K.H.; Li, J.; Chen, P. Facile synthesis of graphene quantum dots from 3D graphene and their application for Fe³⁺ sensing. *Adv. Funct. Mater.* **2014**, *24*, 3021–3026. [[CrossRef](#)]



© 2018 by the authors. Licensee MDPI, Basel, Switzerland. This article is an open access article distributed under the terms and conditions of the Creative Commons Attribution (CC BY) license (<http://creativecommons.org/licenses/by/4.0/>).